AD-763 184

MEASURING SOIL PROPERTIES IN VEHICLE
MOBILITY RESEARCH. REPORT 5. RESISTANCE
OF FINE-GRAINED SOILS TO HIGH-SPEED
PENETRATION

Gerald W. Turnage

Army Engineer Waterways Experiment Station
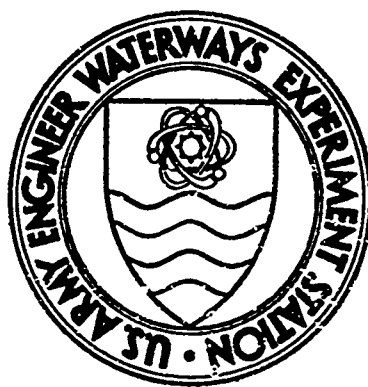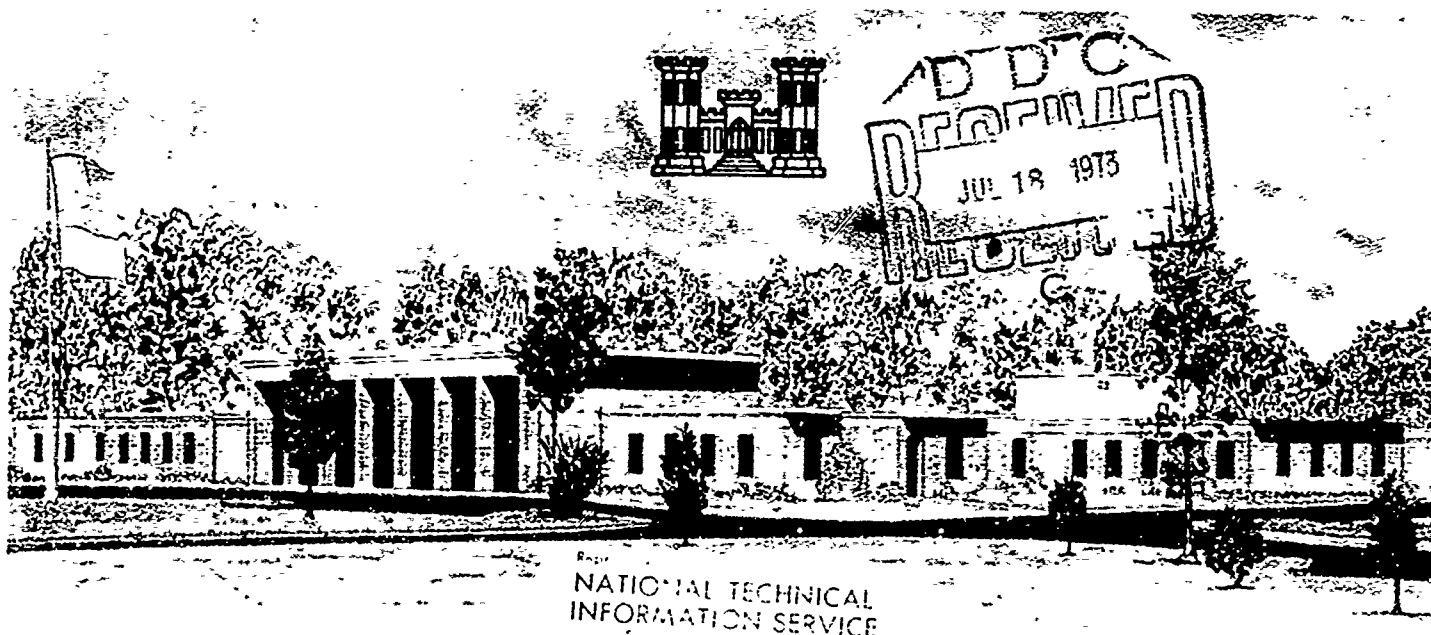Vicksburg, Mississippi

June 1973

TECHNICAL REPORT NO. 3-652

MEASURING SOIL PROPERTIES IN VEHICLE MOBILITY RESEARCH

Report 5

RESISTANCE OF FINE-GRAINED SOILS TO HIGH-SPEED PENETRATION

by

G. W. Turnage

JUL 18 1973

NATIONAL TECHNICAL
INFORMATION SERVICE

June 1973

DOCUMENT CONTROL DATA - R & D

(Security classification of title, body of abstract and indexing annotation must be entered when the overall report is classified)

1. ORIGINATING ACTIVITY (Corporate author)	2a. REPORT SECURITY CLASSIFICATION
U. S. Army Engineer Waterways Experiment Station Vicksburg, Mississippi	Unclassified
	2b. GROUP

3. REPORT TITLE

MEASURING SOIL PROPERTIES IN VEHICLE MOBILITY RESEARCH; Report 5, RESISTANCE OF FINE-GRAINED SOILS TO HIGH-SPEED PENETRATION

4. DESCRIPTIVE NOTES (Type of report and inclusive dates)

Report 5 of a series

5. AUTHOR(S) (First name, middle initial, last name)

Gerald W. Turnage

6. REPORT DATE	7a. TOTAL NO. OF PAGES	7b. NO. OF REFS
June 1973	78	11
8a. CONTRACT OR GRANT NO.	9a. ORIGINATOR'S REPORT NUMBER(S)	
b. PROJECT NO. 4A061101A91D	Technical Report No. 3-652 Report 5	
c.	9b. OTHER REPORT NO(S) (Any other numbers that may be assigned this report)	
d.		

10. DISTRIBUTION STATEMENT

Approved for public release; distribution unlimited.

11. SUPPLEMENTARY NOTES	12. SPONSORING MILITARY ACTIVITY
	Assistant Secretary of the Army (R&D) Department of the Army Washington, D. C.

13. ABSTRACT

Vertical penetration tests were conducted in three highly saturated, fine-grained soils—a fat clay, a lean clay, and a silt—with metal probes of six shapes—30-deg-apex-angle, right circular cones; flat circular plates; and flat rectangular plates with width-to-length ratios of 1:1, 1:2, 1:4, and 1:8. Probe sizes ranged from 0.323 to 59.1 sq cm; penetration velocities from 6 to 1221 cm/sec; and soil strengths (in terms of standard cone penetration resistance C_s) from 90 to 2315 kPa. Equations $C_{xs} = 1.0(V/t)_{xs}^{0.100}$ and $P_{xs} = 0.80(V/t)_{xs}^{0.100}$ adequately describe the viscous behavior of the two clays, and $C_{xs} = 1.0(V/t)_{xs}^{0.080}$ and $P_{xs} = 0.95(V/t)_{xs}^{0.100}$ serve this purpose for silt. (C_{xs} and P_{xs} are C_x/C_s and P_x/C_s, respectively, the ratio of soil penetration resistance per unit area of probe base for any given cone or plate, respectively, at any given velocity to that for the 3.23-sq-cm cone at 3.05 cm/sec. $(V/t)_{xs}$ is $(V_x/t_x)/(V_s/t_s)$, where V_x is penetration velocity of the probe that produced C_x or P_x, t_x is square root of the base area of that probe, $V_s = 3.05$ cm/sec , and $t_s = \sqrt{3.23 \text{ cm}^2} = 1.80$ cm.) No noticeable inertial effects were produced in these tests. Plate penetration tests conducted horizontally at speeds to 27.39 m/sec in muddy clays at the Battelle Institute, Frankfurt, Germany, produced soil lift forces strongly affected by inertial effects. These effects are described by an improved dimensionless lift coefficient versus plate-soil numeric (z_g) logarithmic relation that effectively accounts for the influence of penetration velocity and plate inclination angle.

DD FORM 1473, 1 NOV 65 REPLACES DD FORM 1473, 1 JAN 64, WHICH IS OBSOLETE FOR ARMY USE.

14. KEY WORDS	LINK A		LINK B		LINK C	
	ROLE	WT	ROLE	WT	ROLE	WT
Fine-grained soils						
Mobility						
Penetration resistance						
Penetration tests (soils)						
Soil penetration						
Soil properties						
Vehicles						

FOREWORD

The study reported herein was funded by Department of the Army Project 4A061101A91D, "In-House Laboratory Independent Research," sponsored by the Assistant Secretary of the Army (R&D). The study was conducted during 1971-72.

The project was conceived by Mr. G. W. Turnage of the Mobility Research and Methodology Branch (MRMB), Mobility Systems Division, Mobility and Environmental Systems Laboratory (MESL), at the U. S. Army Engineer Waterways Experiment Station (WES). The high-speed loading device used in the project was constructed under contract by WNRE, Inc., Chestertown, Md. The test program was accomplished by personnel of the MRMB under the general supervision of Mr. W. G. Shockley, Chief of the MESL, and under the direct supervision of Mr. S. J. Knight, former Chief of the MRMB, now retired. The report was prepared by Mr. Turnage.

Special acknowledgment is made to Dr. Dieter Schuring, Cornell Aeronautical Laboratory, Buffalo, N. Y., for furnishing the author with certain data used in this report, which were obtained from tests conducted at the Battelle Institute, Frankfurt, Germany, and for his permission to use these data.

COL Ernest D. Peixotto, CE, was Director of the WES during the study and the preparation of this report. Mr. F. R. Brown was Technical Director.

iii

CONTENTS

Preceding page blank

NOTATION

a,b	Intercept and coefficient, respectively, in the equation $F_L = a + bV_x^2$
A	Area of the frontal face of a penetrating body
A_x	Area of the frontal face of a body projected normal to the direction of penetration
C	Soil cohesion measured with a simple shear box (Battelle Institute data)
C_i	Dimensionless inertial lift coefficient
C_L	Dimensionless total lift coefficient
C_s	Average standard soil penetration resistance obtained by penetrating the soil at 3.05 cm/sec with a 30-deg-apex-angle, right circular cone and dividing the average soil penetration resistance (in newtons) by the base area of the cone (3.23 cm^2) and converting the value to kilopascals
C_x	Average soil penetration resistance, a measure obtained in the same way as C_s, except that no restriction is placed on the size of the cone or the penetration velocity used
C_{xs}	Nondimensional cone penetration resistance ratio, i.e. C_x/C_s
$C_{xs}/\left[(V/\ell)_{xs}\right]$	Apparent coefficient of viscosity ratio of a cone
d_s, d_x	Diameter of the base of the standard cone, 2.03 cm, and diameter of the base of any circular-base-area cone or plate, respectively
F	Soil resistance force in the direction of penetration
F_i, F_L, F_v	Inertial lift force, total lift force, and viscous lift force, respectively
ℓ_s, ℓ_x	Square root of base area of the standard cone, 1.80 cm, and square root of A_x, respectively

n Exponent in an equation of form C_{xs} (or P_{xs}) $= q(V/\ell)^n_{xs}$

N_R Reynolds number, the ratio $\dfrac{F_i}{F_v}$. (In this report, F_i as the numerator of N_R is defined as $F_i = \left(\rho A_x V_x^2\right)/2$ rather than $F_i = \left(C_i \rho A_x V_x\right)/2$, i.e. C_i is omitted.)

P_x Average soil penetration resistance force divided by the base area of the plate for any size or shape of flat plate at any penetration velocity

P_{xs} Nondimensional plate penetration resistance ratio, i.e. P_x/C_s

$P_{xs}/\left[(V/\ell)_{xs}\right]$ Apparent coefficient of viscosity ratio of a plate

q Coefficient in an equation of form C_{xs} (or P_{xs}) $= q(V/\ell)^n_{xs}$

V_s/d_s Standard, constant penetration velocity-to-cone base diameter ratio, $(3.05\ cm/sec)/2.03\ cm = 1.50\ sec^{-1}$

V_s, V_x Standard penetration velocity of a cone, 3.05 cm/sec, and any penetration velocity (of a probe of any shape), respectively

V_x/d_x Penetration velocity-to-base diameter ratio for any circular-base-area probe (may take any value)

$(V/d)_{xs}$ Velocity ratio, the ratio of V_x/d_x to V_s/d_s

$(V/\ell)_{xs}$ Velocity ratio, the ratio of V_x/ℓ_x to V_s/ℓ_s; for circular-base-area probes, $(V/\ell)_{xs} = (V/d)_{xs}$

α Inclination angle of frontal face of a body measured relative to the direction of penetration

γ_d Unit dry weight of the soil, kN/m^3

ρ Density of the soil

CONVERSION FACTORS, METRIC TO BRITISH UNITS OF MEASUREMENT

Metric units of measurement used in this report can be converted to British units as follows:

Multiply	By	To Obtain
meters	3.281	feet
centimeters	0.3937	inches
square centimeters	0.1550	square inches
kilonewtons	224.8	pounds (force)
kilonewtons per cubic meter	6.366	pounds per cubic foot
kilopascals	0.1450	pounds per square inch
kilograms	2.205	pounds (mass)
kilometers	0.6214	miles (statute)

SUMMARY

Vertical penetration tests were conducted in three soils--a fat clay, a lean clay, and a silt--at 90 percent or higher saturation with probes of six shapes--30-deg-apex-angle, right circular cones; flat circular plates; and flat rectangular plates with width-to-length ratios of 1:1, 1:2, 1:4, and 1:8--and sizes from 0.323 to 58.1 cm^2. Penetration velocities ranged from 5.82 to 1221 cm/sec. Viscous behavior of the three soils was similar to that of a pseudoplastic fluid. For both clays, $C_{xs} = 1.00(V/\ell)_{xs}^{0.100}$ and $P_{xs} = 0.80(V/\ell)_{xs}^{0.100}$ adequately described this behavior for all cones and all plates, respectively. (C_{xs} and P_{xs} are C_x/C_s and P_x/C_s, respectively. They define the ratio of soil penetration resistance per unit area of probe base for any given cone or plate, respectively, at any given velocity, to that for the 3.23-cm^2 cone at 3.05 cm/sec. $(V/\ell)_{xs}$ is velocity ratio, $(V_x/\ell_x)/(V_s/\ell_s)$, where V_x is penetration velocity of the probe that produced C_x or P_x, ℓ_x is the square root of the base area of that probe. $V_s = 3.05$ cm/sec, and $\ell_s = \sqrt{3.23 \ cm^2} = 1.80$ cm.) For the silt, $C_{xs} = 1.00(V/\ell)_{xs}^{0.080}$ and $P_{xs} = 0.95(V/\ell)_{xs}^{0.100}$ appear better-suited to describing soil viscous behavior under cone and plate penetrations, respectively. No noticeable inertial effects were produced in these tests, although velocities to 1221 cm/sec and velocity ratio values to 1134 were developed.

Inertial effects strongly influenced total soil lift force in plate penetration tests conducted horizontally in muddy clays at the Battelle Institute, Frankfurt, Germany. These effects were described by a dimensionless lift coefficient (C_L) versus plate-soil numeric (π_s) logarithmic relation that is conceptually similar to the C_L versus N_R

Preceding page blank

(Reynolds number) relation often used in fluid mechanics for this purpose. Separation of data in the C_L versus π_s relation by values of inclination angle α was eliminated by using area A_x projected normal to the direction of penetration instead of plate base area A in the term $\left(\rho A_x V_x^2\right)/2$ that appears in both C_L and π_s. Data were not available, however, to demonstrate conclusively that the C_L versus π_s relation is independent of plate size over the full range of values of π_s. Also, the C_L versus π_s relation separates by levels of soil cohesion C (measured under near-static conditions with a simple shear box).

It is not unusual for vehicles operating in fine-grained soils to develop significant forces attributable to soil viscosity, and dynamic probe testing (air-dropped penetrometers, for example) could well develop very large soil inertial forces. Interpretation of the C_L versus π_s relation showed that only in extreme circumstances will soil-vehicle interactions develop significant soil inertial forces (possible exceptions--some aircraft landings and takeoffs, ground vehicles operating in or near the swimming mode).

Further plate penetration tests are needed in very weak, saturated, fine-grained soils to: (a) verify independence of the C_L versus π_s relation on plate size over a wide range of values of π_s, and (b) define a measure of soil strength suitable for eliminating separation of the C_L versus π_s relation by levels of soil strength.

MEASURING SOIL PROPERTIES IN VEHICLE MOBILITY RESEARCH

RESISTANCE OF FINE-GRAINED SOILS TO HIGH-SPEED PENETRATION

PART I: INTRODUCTION

Background

1. A prime consideration in evaluating a soil for most engineering purposes is the ability of the soil to withstand the forces to be imposed on it. Over the years effective techniques have been developed for predicting the behavior of soils under static or near-static loading (dams, foundations, etc.) and under transient loading spread over a large surface area (roadbeds for paved highways, airfields, etc.). The resistance of soils to localized, high-speed penetration has received relatively little attention, however, and no widely recognized technique exists for predicting soil behavior under this type of loading.

2. Improved understanding of soil response during high-speed loading will advance the development of several techniques presently limited by only general knowledge of this phenomenon. In particular, the ability to predict the response of soils to the dynamic load imposed by the running gear of a land-based vehicle would lead to better-defined criteria for building unsurfaced roadways and for predicting vehicle performance on such roads. Similarly, the design of unsurfaced airfields and the prediction of aircraft landing gear performance on these fields would be improved. These applications imply obtaining soil strength measurements under conditions of moderate-speed soil penetration and extrapolating them to the high-speed condition by use of the relati sought in this study. Conversely, another application would be the prediction of soil strength for a moderate-penetration-speed condition from measurements taken remotely at high penetration speed—by an air-dropped penetrometer, for example.

3. To be most useful, especially in the field, the resistance of soils to high-speed penetration should be related to some standard

1

measurement of soil penetration obtained by an appropriate field device.
The penetration resistance of a standard cone was selected as the datum
because (a) its value can be obtained by a simple, hand-operated pene-
trometer and (b) the U. S. Army Engineer Waterways Experiment Station
(WES) has successfully correlated such measurements with the performance
of vehicles moving slowly (at 5 km/hr* or less) in fine-grained soil.[1,2]
Tests of vehicles operating at higher speeds (to about 20 km/hr) indi-
cate that these correlations must be refined when higher speeds are con-
sidered.[3] A first step in this refinement is to obtain a basic und ~-
standing of the response of soils to changes in the velocity, size, and
shape of the element penetrating the soil at high speeds.

4. In a previous study,[4] WES examined the effects on the penetra-
tion resistance of near--saturated, fine-grained soils of probe size,
shape, and velocity within a limited range of values of each of the per-
tinent variables. Two probe shapes were used: flat, circular plates
and 30-deg-apex-ang`', right circular cones. Near-constant vertical
test velocities ranged from 0.001 to 35 cm/sec. Horizontal, constant-
acceleration tests were also made at speeds to 450 cm/sec, but the rela-
tion of penetration force to velocity was obscured by variations in soil
strength over the length of the soil test beds used.

5. The fine-grained test soils in that study[4] behaved as pseudo-
plastic materials whose changes in penetration resistance were attribut-
able almost entirely to viscous effects.** A broader range of test
conditions is examined in the study reported herein, including some
conditions in which inertial as well as viscous phenomena contribute
significantly to overall soil penetration resistance.

---

* A table of factors for converting metric units of measurement to
  British units is given on page ix.
** In reference 4 and throughout this report, the term viscosity de-
  scribes the physical property of a material (in this case, a satu-
  rated, fine-grained soil) that enables it to develop a shearing
  stress whose magnitude depends on the rate of shear (or velocity
  gradient) associated with penetration of the material by a probe.

Purposes and Scope

6. The purposes of this study were to:

   a. Develop and examine, respectively, relations that describe viscous and inertial effects on soil penetration resistance for a variety of probe sizes, shapes, and penetration velocities.

   b. Compare the relations developed in a above with those of behavioral models from rheology and from fluid mechanics.

   c. Discuss the application of relations from a above to real-world situations, i.e. soil-vehicle interactions, dynamic probe testing, etc.

7. Penetration tests were conducted in three fine-grained soils-- a fat clay, a lean clay, and a loessial silt--with probes of three general and six specific shapes: 30-deg-apex-angle, right circular cones; flat, circular plates; and flat, rectangular plates with width-to-length ratios of 1:1, 1:2, 1:4, and 1:8. Sizes of probe base areas ranged from 0.323 to 58.1 cm^2. Soil was mixed with the desired amount of water and compacted to produce highly saturated, homogeneous mixtures of various strengths. Test penetration rates ranged up to 1221 cm/sec.

PART II: TEST PROGRAM

Soils and Their Preparation

Soils

8. The three soils tested were classified according to the Uni-
fied Soil Classification System as fat clay (CH), lean clay (CL), and
silt (ML) with plasticity indexes of 38, 16, and 5, respectively
(fig. 1). The fat clay was a Mississippi River alluvium found in the
Long Lake area northwest of Vicksburg, Mississippi; the lean clay was
from the WES grounds; and the silt was a loess from a borrow pit about
5 km north of Vicksburg.

9. In general, fine-grained soils that are prepared to a high
degree of saturation and tested to failure under undrained conditions
exhibit little or no frictional strength. Undrained triaxial compres-
sion tests have shown that the shear resistance of given samples of both
highly saturated fat and lean clays was essentially constant over a wide
range of confining pressures and normal loads, and the soils could be
considered as purely cohesive with no frictional component.[5] Also,
Smith[6] has shown that there exists a well-defined linear relation be-
tween standard penetration resistance and cohesion for each of these
soils when they are saturated to 90 percent or more.

Soil preparation

10. Nearly all tests in fat clay were made in 0.8- by 1.6- by
8.2-m soil cars. Three soil car test sections were used which had al-
ready been prepared to approximately 95 percent saturation by the pro-
cedures described in reference 7. Combinations of moisture content and
unit dry weight used to produce these test sections are shown in fig. 2a.
For each test section, a closed symbol represents the average value of
moisture content and dry density used to attain approximately 95 percent
saturation. The relation of standard penetration resistance C_s to
moisture content for fat clay is represented by the rightmost curve in
fig. 3 and is based on data accumulated over a long period in process-
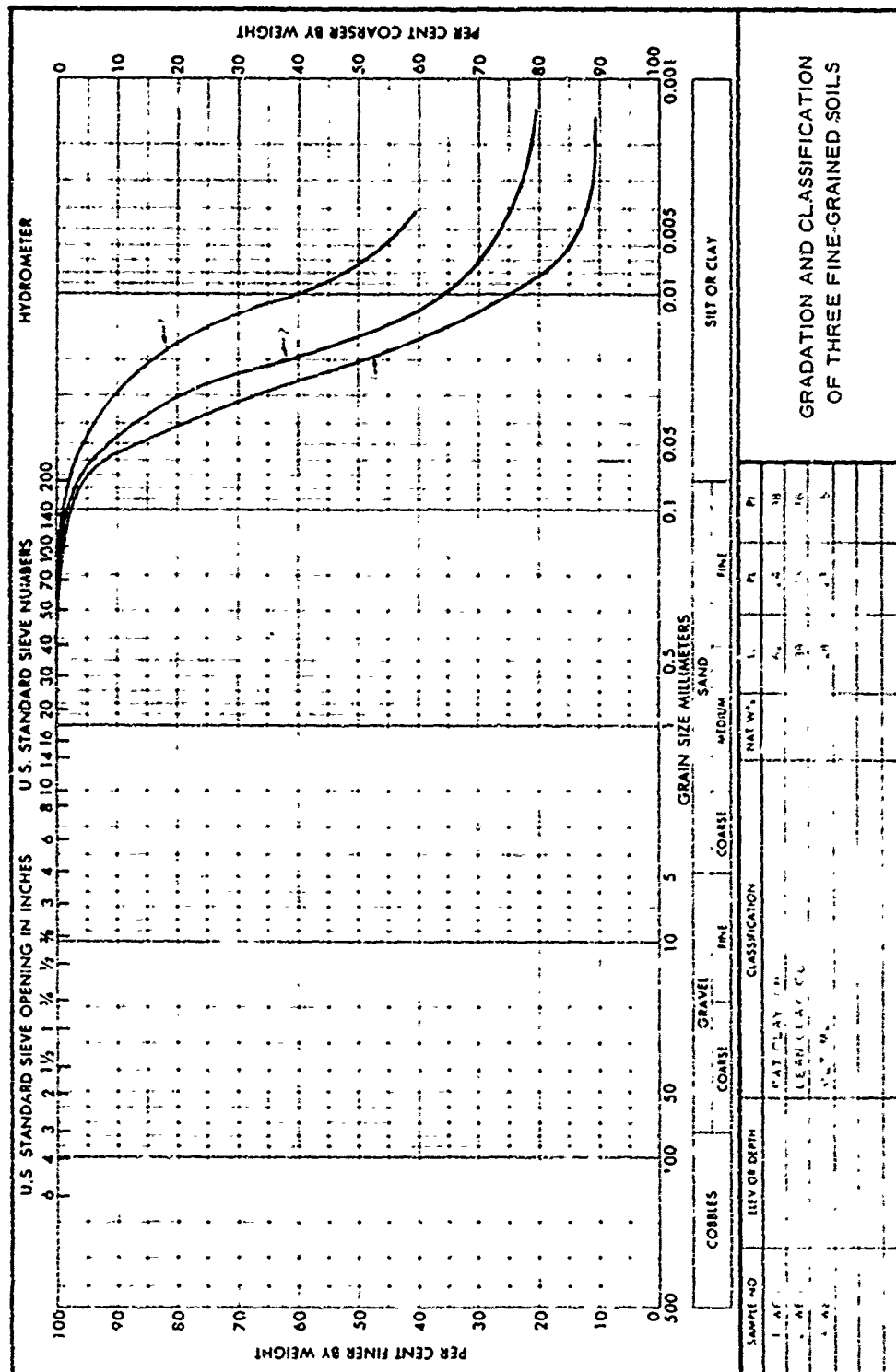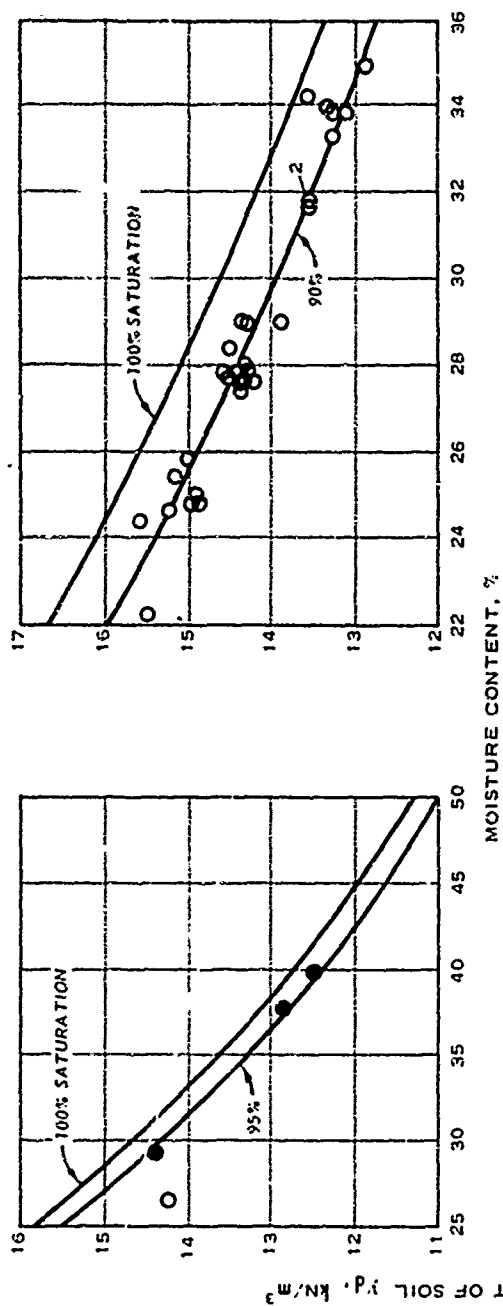ing this material in soil cars. The proximity to the curve of the three

4

Fig. 1. Gradation and classification data

Fig. 2. Relation of unit dry weight to moisture content, three fine-grained soils

NOTE: EACH OPEN AND CLOSED CIRCLE REPRESENTS THE AVERAGE OF DATA FROM THREE SAMPLES IN ONE SOIL MOLD OR ONE SOIL CAR. RESPECTIVELY.
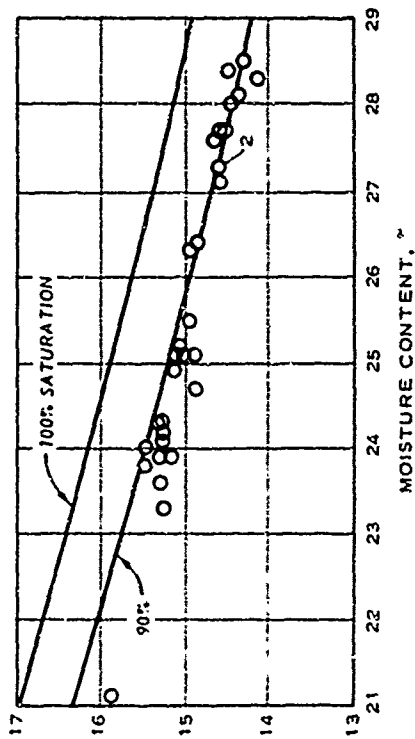
6

NOTE: EACH OPEN AND CLOSED SYMBOL REPRESENTS THE
AVERAGE OF DATA FROM THREE SAMPLES IN ONE
SOIL MOLD OR ONE SOIL CAR, RESPECTIVELY.
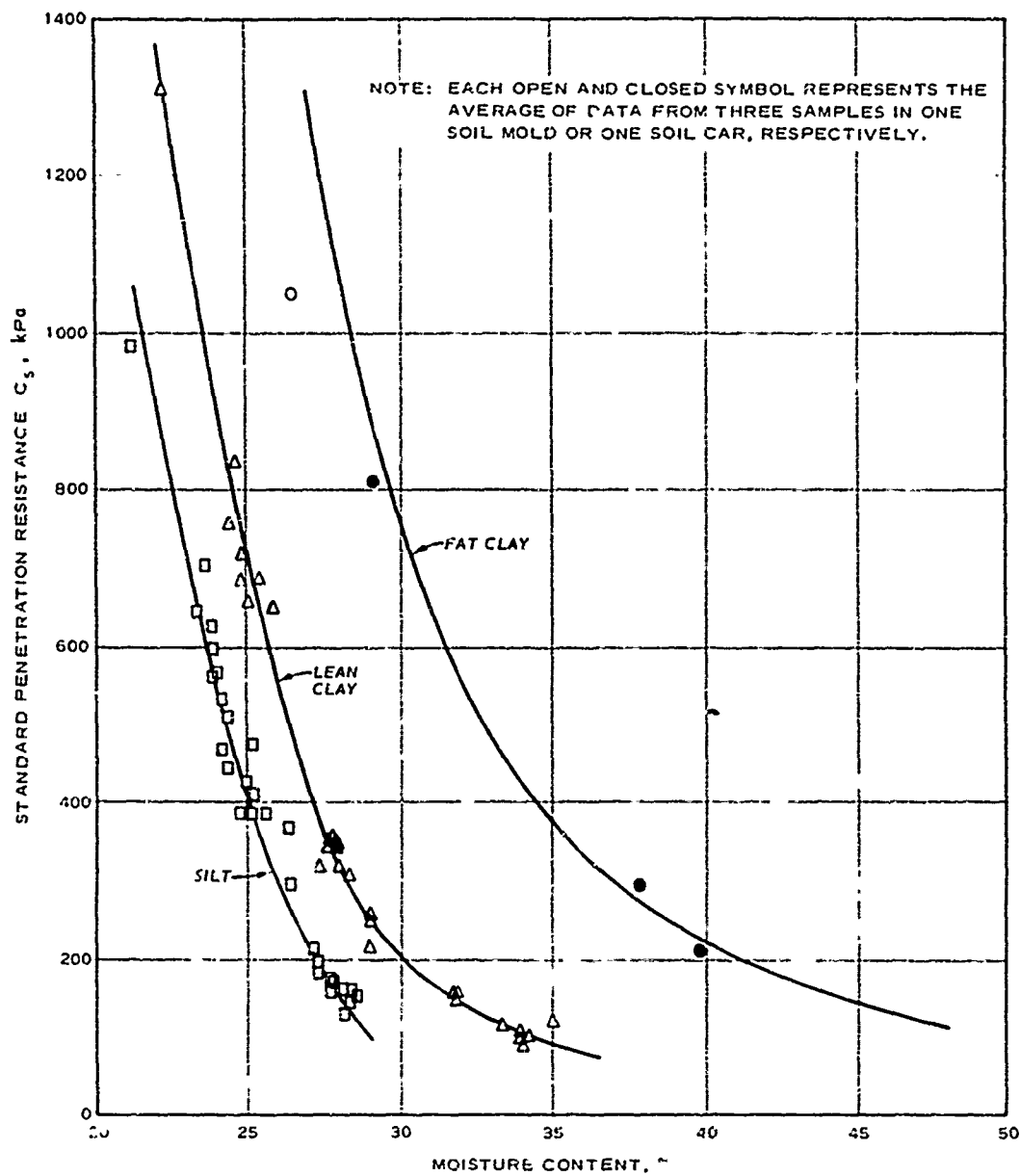
Fig. 3. Effect of moisture content on penetration resistance;
3.23-cm^2-base-area cone, 3.05-cm/sec penetration velocity,
95 percent-saturated fat clay, 90 percent-saturated lean clay
and silt

7

closed symbols (one each for the three soil car test sections used in this study) indicates that a test section of fat clay can be prepared about to a given value of C_s by mixing the soil at a predetermined moisture content and then compacting it. Note, however, from the shape of the curve that the value of C_s* becomes increasingly sensitive to moisture content as the value of moisture content decreases.

11. A few of the tests in fat clay and all of the tests in lean clay and in silt were conducted on soil samples contained in 39.4-cm-diam steel molds. Soil for these molds was prepared in a small, single-shaft pug mill with extrusion attachment.[6] Usually sufficient soil was mixed at one time to prepare three or more molds. For most of the tests in molds, the container was composed of a base and two cylinders, each 17.8 cm high, rigidly attached to form one unit. For a few tests of small probes at low velocity, the top cylinder was replaced by a 5.1-cm-high cylindrical collar. A mold test sample was built in 5-cm layers, each compacted by 120 blows of a 13.2-kg hammer falling 15 cm. After the top layer was compacted, the soil was trimmed to the top of the mold, the mold was tightly covered with an impervious membrane, and the soil was allowed to cure until reasonable moisture equilibrium was attained. Curing time varied from about 1 hr for the silt to about 24 hr for the fat clay. Combinations of moisture content and dry density used to produce soil samples for the three test soils are shown in fig. 2. Open symbols represent the average values from soil test molds. Soil preparation procedures produced approximately 90 percent saturation in the molds for all three soils. In fig. 3, the curves that describe the

---

* C_s is the resistance of soil to penetration of the standard WES cone, at a standard penetration rate, expressed in kilopascals (see page ix). In WES field trafficability work (see references 1 and 2), penetration resistance of the same WES cone is used as an index of effective field soil strength as seen by vehicles. To avoid the implication that the cone in this use measures a specific engineering property of the soil, it is customarily stated simply as the cone index (CI) without stated dimensions, even though it is calibrated in terms of load (pounds) per unit of cone base area (square inches). Thus, while philosophically different, the cone index of soils is in fact simply related to C_s through a straightforward dimensional conversion, i.e. $CI = 0.1450 C_s$.

relation of standard penetration resistance to moisture content for the silt and the lean clay are based on the data shown, and data for these two soils cluster fairly closely about their respective curves. The curve shown for fat clay, on the other hand, is based on soil car test sections more nearly at 95 percent saturation (paragraph 10). The open-symbol data point (fig. 2a) for the single fat clay test mold (prepared to about 90 percent saturation) lies somewhat below the curve, as would be expected.

Test Apparatus

Cones and plates

12. The cones and plates used in this study are shown in fig. 4. The following tabulation characterizes the probe shapes and sizes.

		Probe Base Size			
		Dimensions, cm			Area
No.	Probe Shape	Diameter	Width	Length	cm^2
1	Right circular cone	1.28	--	--	1.29
2		2.03	--	--	3.23
3		4.05	--	--	12.9
4		5.73	--	--	25.8
5		8.60	--	--	58.1
6	Flat circular plate	1.28	--	--	1.29
7		2.03	--	--	3.23
8		4.05	--	--	12.9
9		5.73	--	--	25.8
10		8.60	--	--	58.1
11	Flat rectangular	--	1.27	1.27	1.61
12	plate (1:1 width-	--	2.54	2.54	6.45
13	to-length)	--	5.08	5.08	25.8
14		--	7.62	7.62	58.1
15	Flat rectangular	--	1.27	2.54	3.23
16	plate (1:2 width-	--	3.59	7.18	25.8
17	to-length)	--	5.39	10.78	58.1
18	Flat rectangular	--	1.27	5.08	6.45
19	plate (1:4 width-	--	2.54	10.16	25.8
20	to-length)	--	3.81	15.24	58.1
21	Flat rectangular	--	1.27	10.16	12.9
22	plate (1:8 width-	--	1.80	14.37	25.8
23	to-length)	--	2.70	21.56	58.1
24	Right circular cone	0.641	--	--	0.323

9
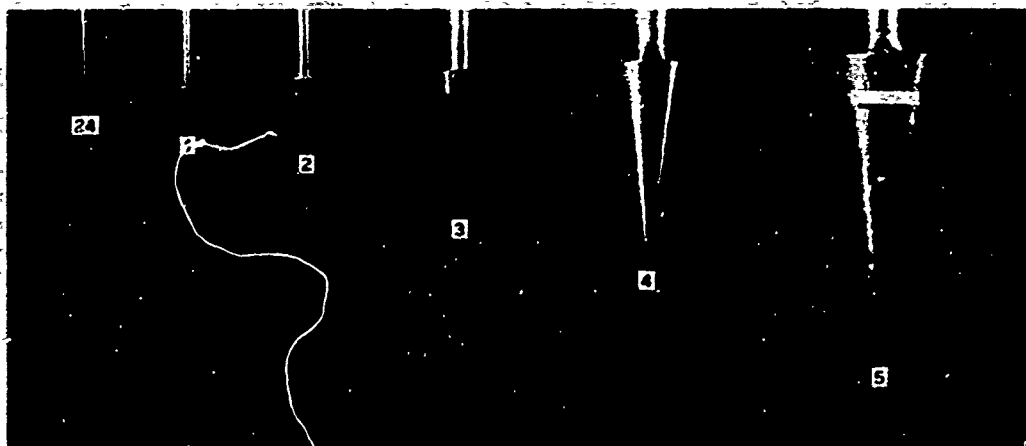
a. 30-DEG-APEX-ANGLE, RIGHT CIRCULAR CONES
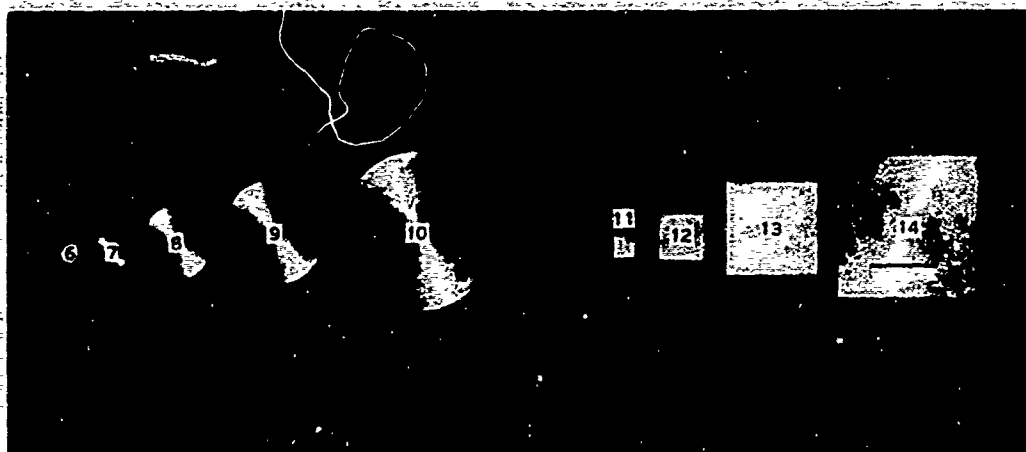
b. FLAT CIRCULAR AND RECTANGULAR (1:1) PLATES
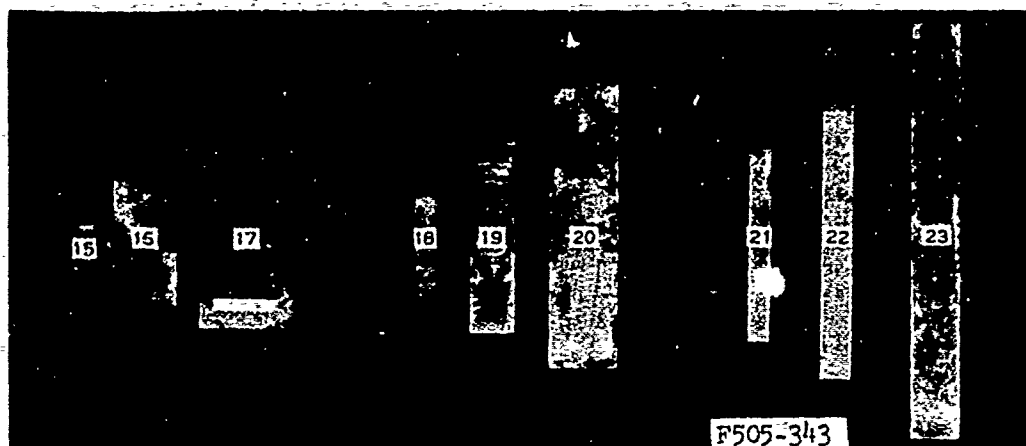
c FLAT RECTANGULAR (1:2, 1:4, AND 1:8) PLATES

Fig. 4. Test cones and plates

The nominal penetration velocities were designated as follows:

No.	Nominal Velocity cm/sec
1	3.05
2	10
3	30
4	100
5	300
6	1000
7	1300

13.   Each probe was of one-piece steel construction, and consisted of a probe head (cone or flat plate) and a shaft. The shafts were strong enough to ensure straight alignment (no flexure) and small enough to prevent soil drag for at least 15-cm penetration beyond the probe base. (The only exception was probe 24, whose shaft was 0.3 cm in diameter for 8 cm upward from the cone base and 0.9 cm in diameter over its remaining length.) Each probe was 41 cm long overall. The upper end of each shaft was threaded to connect it to a force-measuring load cell (fig. 5).
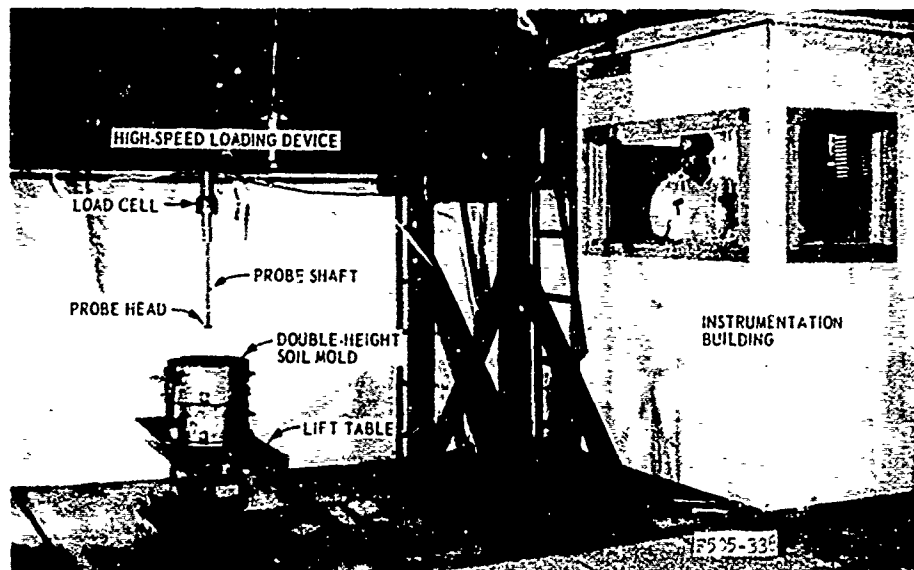
Fig. 5.   General view of high-speed loading device, soil mold, and instrumentation building

Penetration devices

14. **High-speed loading device.** The powerful and versatile loading device shown in fig. 5 allows loads, large or small, to be applied to test specimens (tires, shock absorbers, soils, etc.) at controlled velocities for preset single strokes adjustable from 10 to 30 cm. Design velocities range from near zero to about 1300 cm/sec. The characteristic travel-versus-time curve for the active plunger of this device is S-shaped. During the early part of the stroke the plunger is accelerated from rest to a preset velocity; over the middle portion of the stroke, velocity remains constant (within ± 10 percent); and near the end of the stroke, the plunger is rapidly decelerated to zero velocity. When operating at full 30-cm stroke, the portion of the total stroke that remains within ± 10 percent of constant speed ranges from about 90 percent for speeds of the order of 10 cm/sec and drops to about 20 percent at maximum speed. In practice, maximum velocity attainable proved to be 1221 cm/sec, rather than the design value of 1300 cm/sec. While this limitation had negligible influence on the present study, modifications are under way to increase the attainable velocity and, more importantly, to increase the length of stroke that falls within the ± 10 percent of constant speed criterion at the higher speeds.

15. For test velocities up to 300 cm/sec, conventional column-type load cells were used to measure the resistance of soil to penetration. The very large forces associated with both the acceleration and the deceleration phases of penetrations at larger peak velocities required that penetration resistance be measured by a special low-mass, web-type load cell with mechanical restraint to prevent destructive overload. In each test with the high-speed loading device, an accelerometer mounted just above the load cell measured acceleration during each penetration (fig. 5).

16. **Low-speed penetrometer.** For all tests in molds (except the first few in lean clay),* penetrations to measure standard soil

---

* C_S measurements in the first few molds of lean clay and in all tests of fat clay in the soil cars were made with the high-speed loading device. Penetration velocities to obtain C_S varied somewhat with the

penetration resistance C_s were made with a mechanical, low-speed laboratory penetrometer with which standard penetration velocity (3.05 cm/sec) can be repeated with an accuracy of ± 1 percent.

Test Procedures and Data Reduction

Procedures common to all tests

17. <u>Data recorded.</u> Testing involved the measurement of soil penetration resistance forces, as a function of penetration and velocity of penetration, in a situation where system inertial forces were at times large, even during the near-constant velocity segment of the penetration stroke that was of interest. To preserve resolution in recording the soil forces, a special technique was used to subtract from the overall force signal a signal proportional to those forces due to acceleration of the probe, shaft, and load cell which passed through the ad cell, thereby allowing soil penetration forces per se to be recorded directly. During each stroke, three separate signals were continuously recorded: (a) accelerometer output, (b) load cell output, and (c) force signal (b) corrected for acceleration (a). Before each test or series of tests with a given probe at a given velocity, the high-speed loading device was exercised by moving the probe downward in air (i.e. with zero penetration resistance) at the test design velocity. In-air runs were repeated until, by adjusting potentiometer settings that controlled the correction signal from signal a, the contribution of inertia to signal c was eliminated and the value of signal c remained constant at zero throughout the in-air run. During the subsequent in-soil test, signal c measured soil resistance force free of the effects of acceleration and deceleration of the probe-load cell assembly. Hereafter, the term "soil

---

device, from a low of 1.66 cm/sec to a high of 4.51 cm/sec. Equation 4, paragraph 37, was used to adjust measured C_s (actually C_x) to C_s at 3.05 cm/sec. This adjustment was never more than 6 percent, and usually less than 3 percent.

13

penetration resistance" is the in-soil force measured by signal c. Records of the relatively low resolution signals a and b were used only for spot checks and backup. Two other variables were electrically recorded: probe velocity and depth of the probe relative to the soil surface. (Zero depth was the point where the probe base was flush with the original soil surface.)

18. The five electrical test signals were recorded on analog magnetic tape and later machine-digitized at 1-cm penetration intervals. The computer printout of each digitized test record was marked by hand to show the range of acceptable readings. (Criteria for data acceptability are described in paragraph 20.) For each test, an average value was then determined for each of the five signals. For duplicate or triplicate tests, the final value reported for a given variable is the average of the two or three average values from the separate penetrations.

19. **Data acceptability.** In the usual cone penetration test, the first, or surface, reading is that taken when the base of the cone is flush with the soil surface (i.e. at a tip penetration depth equal to the cone height). For fine-grained soils a descriptive index of penetration resistance is then determined by averaging the near-constant penetration resistance values obtained within a specified soil layer, and dividing this average value by the base area of the cone. For the 3.23-cm^2 cone at 3.05 cm/sec, this index is termed standard cone penetration resistance C_s ; for a cone of any other size and/or penetration velocity, it is C_x . In similar manner, P_x is defined as the average of the near-constant penetration resistance values produced by any one of the flat plates at any particular velocity within a specified soil layer, divided by the plate base area.

20. The primary criterion used to determine the soil layer within which data would be accepted was that this layer contain values of probe penetration velocity and of soil penetration resistance that varied from their average values by no more than ±10 percent. Secondary requirements were that, to the degree possible, the same soil layer (as

determined by measurements from the original soil surface) be used each time, and that this layer be at least 10 cm thick. Simultaneous satisfaction of these requirements was complicated by two major factors. First, the depth of penetration to achieve stable readings of penetration resistance changed as a function of: (a) probe shape and size (acceptable readings for nearly all the cones could be taken starting at the soil surface; for the flat plates, depth to stable readings increased as probe size increased); (b) soil type (tests in silt, but not in either clay, produced noticeable depressions of the soil surface around the probe penetrations, and penetration resistance values stabilized only after the probe base penetrated well below the original soil surface); (c) soil strength (the weaker the soil, the greater the required depth for silt); and (d) penetration velocity (the lower the velocity, the greater the depth for silt). Second, constant penetration velocities (within ±10 percent) were achieved only within part of the 30-cm loading device stroke length, and the length of this part decreased as the value of peak, near-constant velocity increased (paragraph 14).

21. With the factors above taken into account, an acceptable degree of uniformity was achieved in selecting the specified soil layer by using data from the 5- to 15-cm layer whenever these data satisfied the ±10 percent criterion for soil penetration resistance and for probe velocity. When data from this layer did not meet these criteria, data were used from a layer as nearly the same as the 5- to 15-cm layer as possible (and usually overlapping the 5- to 15-cm layer) and as near 10 cm thick as possible, and within which the ±10 percent speed and penetration resistance criteria were satisfied. The overall effect of this procedure was to use test data obtained under stable conditions of penetration resistance and probe velocity within a range f depths similar in terms of both thickness and location. Repeatability of near-constant velocities for duplicate or triplicate tests was on the order of ±2 to 3 percent, so that this factor had negligible influence on the averaged values reported.

15

Tests in soil molds

22. All tests in the lean clay and the silt, and one set in the fat clay,* were conducted in 39.4-cm-diam steel molds. For efficiency and economy, a maximum number of penetrations in each mold was planned. The primary consideration was that each penetration be unaffected by an adjacent penetration or by proximity to either the sidewall or the bottom of the container. As a secondary objective, at least two penetrations were desired for each combination of probe size and shape, penetration velocity, and soil strength, so that an average value relatively unaffected by soil nonuniformities could be obtained. Finally, locations were required in each mold for two or three standard (C_s) penetrations.

23. The three objectives above were satisfied by: (a) making the minimum lateral spacing between any two adjacent penetrations and between any penetration and the sidewall of the test mold at least twice the diameter of the larger cone or circular plate, or the length plus half the width of the larger rectangular plate measured perpendicular to its longer dimension (templates were used to assure accurate location of each penetration in a mold); (b) testing the larger probes last in a given mold; and (c) so adjusting the mold height (see fig. 5) that penetration came no closer to the bottom of the mold than the larger dimension of probe base.

24. Adherence to these guidelines eliminated tests in molds of probes 5 and 10, the largest cone and flat circular plate, respectively. The spacing guidelines were relaxed slightly for probe 23 (2.70 by 21.56 cm) because it was one of only three test plates at 1:8 width-to-length ratio. The guideline regarding depth of penetration was also relaxed for a 25.8- or 58.1-cm^2 probe when it was the last probe tested in a given mold. (Only one penetration per mold was made with the 25.8- and 58.1-cm^2 probes.) In the final analysis of the data, however, no

---

* All routine tests in fat clay were made in three available soil cars. Tests with probe 24 only were made in one mold each of the three test soils at very high soil strength values as part of a special test set discussed in paragraph 44.

16

data were used from tests in which the base of a probe was more than 17 cm beneath the soil surface, so that the penetration depth rule was in fact not violated.

25. At least two and usually three penetrations were made in each mold with the 3.23-cm^2 cone at 3.05 cm/sec in the 5- to 15-cm depth range to obtain values of C_s , which were used to characterize the base-line strength of the test soil. In most cases, the first c   or two C_s measurements were taken before the C_x or P_x measurements, and the last C_s measurement was taken afterwards. No noticeable pattern was found between the values of first and last C_s measurements. Neither was there found a tendency of the second and/or third of duplicate or triplicate C_x or P_x measurements to increase or decrease. Taken together, these observations indicate that the spacings used in the probe tests in molds were adequate. Values of C_s in the soil molds covered a broad range, 90 to 1315 kPa for lean clay and 106 to 983 kPa for silt. C_s for the only mold of fat clay was 1053 kPa (see fig. 3).

Tests in soil cars

26. Each plate and cone (except probe 24) was tested in at least two of the three 0.8- by 1.6- by 8.2-m soil cars of fat clay. Based on all C_s measurements taken in the three cars, average val...s were 210, 290, and 809 kPa, respectively (low, moderately low, and high soil strengths). Tests were conducted by moving a soil car beneath the high-speed loading device (fig. 6), mounting a given probe, zeroing out the effects of probe acceleration (paragraph 17), and penetrating vertically at the desired speed. A single longitudinal lane of tests was developed by rolling the car along steel tracks from one specified test position to the next. A different lane was located by moving the entire loading device laterally on rollers to a new position above the soil car. The same minimum spacing criteria between adjacent penetrations, used in the tests in soil molds, was maintained in tests in the soil cars. Including all tests in the soil cars, each probe was tested at at least five of six nominal test velocities (Nos. 2-7 in paragraph 12).

27. Procedures developed and used for several years at WES to
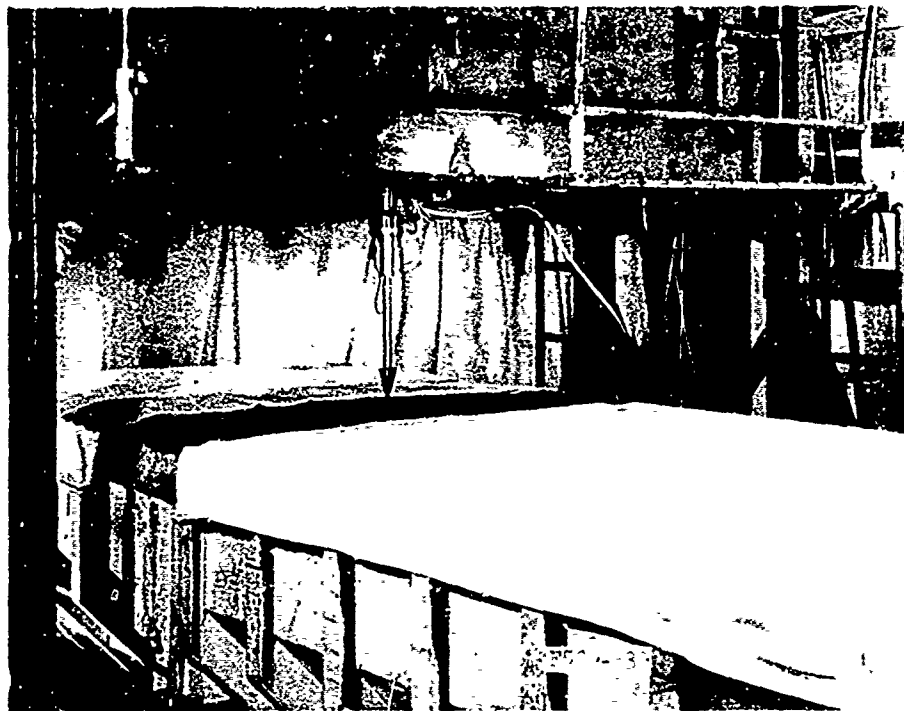
Fig. 6. Soil car in position beneath high-speed loading device

construct soil car test sections of uniform strength were used to build
the three fat clay test sections. In cars as large as those used, the
degree of soil strength uniformity achievable in small test molds is not
possible. Standard deviations of C_s values measured in the three fat
clay test cars were 37.7, 35 5, and 59.1 kPa for the 210, 290, and
809 kPa cars, respectively. Minimizing the influence of variation in
soil strength within a given car was accomplished by conducting at least
duplicate (usually triplicate) consecutive tests within a given lane, by
taking a C_s measurement just ahead of and just beyond each group of
two or three repetitive C_x or P_x penetrations, and by then treating
this gr of C_x (or P_x) and C_s measurements as a unit. This ap-
proach ilted in acceptably low data scatter, as will be seen in the
subsequent analysis.

18

PART III: ANALYSIS OF DATA

Relation of Results Developed Herein
to Results of Earlier Study

28. To set the stage for the analysis of data reported herein, a
brief review of the major findings in an earlier, closely related WES
study[4] is appropriate. The basic aim of chat study was to describe in
useful quantitative form the effects of velocity, size, and shape of
probes on the penetration resistance of fine-grained soils. Relative to
velocity, soil penetration resistance was found to remain constant until
a "threshold penetration velocity" was exceeded. Values of threshold
velocity were quite small and varied both with soil type and cone size
(fig. 7). Beyond the velocities in fig. 7, soil penetration resistance
increased as a power function of penetration velocity. Data at different
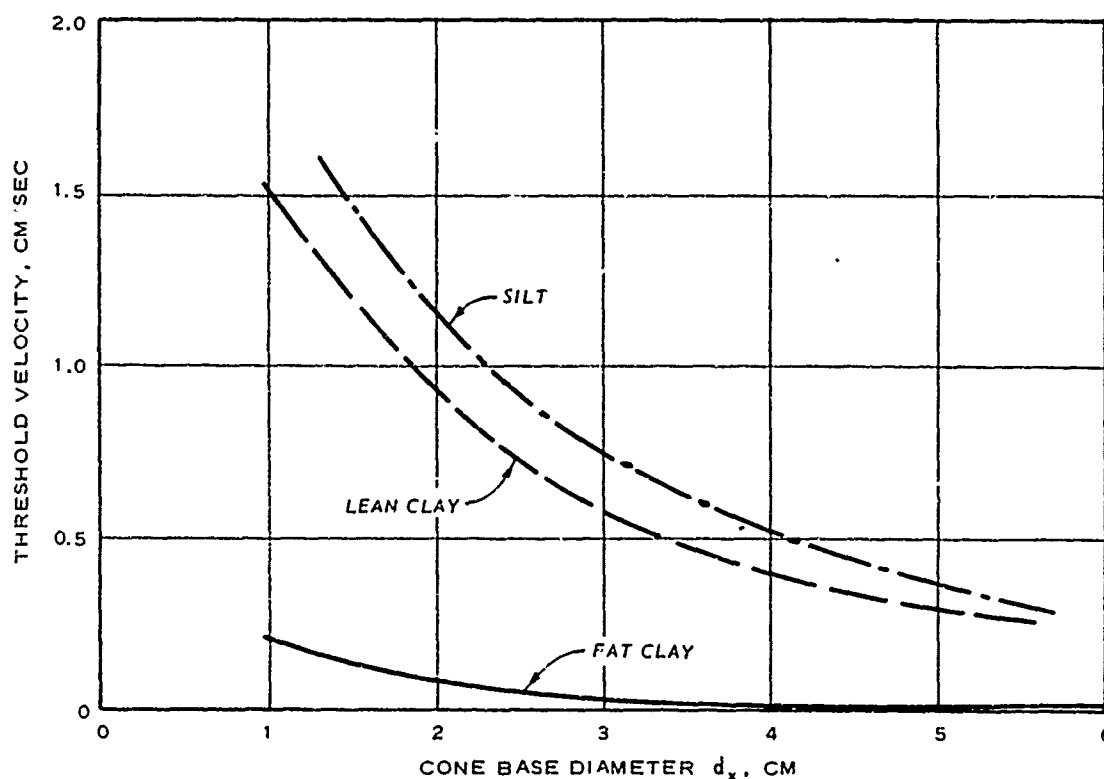
Fig. 7. Influence of cone base diameter on threshold penetration
velocities of three fine-grained soils (from reference 4)

19

soil strengths and for different cone sizes and penetration velocities could be represented by a single curve by expressing dependent soil penetration resistance as the ratio $C_x/C_s = C_{xs}$, and using as the independent variable the ratio of the penetration velocity of the probe to its base diameter V_x/d_x . Note that V_x/d_x may be interpreted as a nominal velocity gradient or rate of shear characterizing the system.

29. This presentation was developed a step further by dividing the independent variable V_x/d_x by the ratio V_s/d_s , standard penetration velocity (3.05 cm/sec) divided by the base diameter (2.03 cm) of the standard cone, to produce the velocity ratio $(V/d)_{xs}$. The earlier tests were run in a fat clay, a lean clay, and a silt. In fig. 8 results of the vertical penetration tests of cones in fat clay are shown in terms of C_{xs} versus $(V/d)_{xs}$, i.e. relating relative penetration resistance as a function of relative rate of shear. The relation in fig. 8 is nondimensional and normalized on the basis of conditions associated with standard cone penetration resistance. Slightly different values of exponent n in the equation in fig. 8 were obtained for the three test soils (0.092, 0.109, and 0.091 for fat clay, lean clay, and silt, respectively). The small differences in values of n suggested that n varies only slightly, if at all, as a function of soil type for near-saturated fine-grained soils. This conclusion was later reinforced by other researchers,[8] whose verification tests of the relation above, over a range of velocity ratio values from 0.1 to 100 in another saturated clay, showed very good data fit for n = 0.100 . For the tests with flat, circular plates in reference 4, the relation $P_{xs} = 0.91(V/d)_{xs}^{0.056}$ described the test data for velocity ratio values from 0.004 to 0.8. (P_{xs} is the soil penetration resistance ratio for plates, P_x/C_s .)

30. The relations C_x versus $(V/d)_x$ and P_x versus $(V/d)_x$ have the same dimensions as shearing stress versus rate of shear, the classic relation that defines a material's coefficient of viscosity, and exhibit the same general shape as curves E or B in fig. 9a. Note that fig. 9a is an arithmetic representation, and that ψ signifies a material's yield value, which relates to the threshold penetration velocity discussed in paragraph 28. For non-Newtonian fluids (i.e. fluids

20
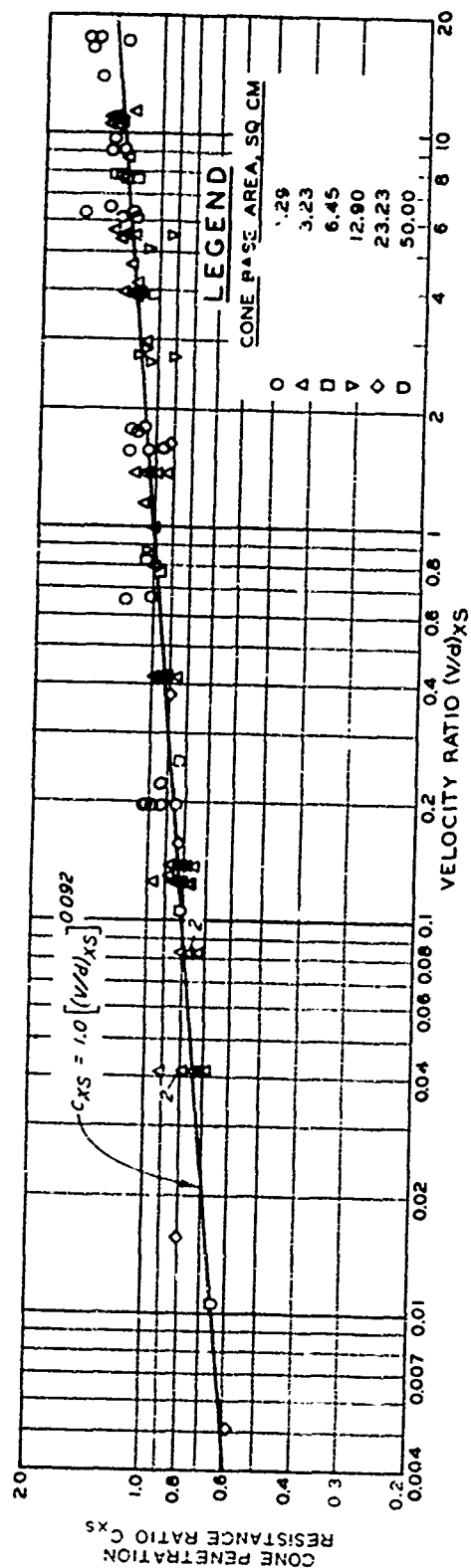
Fig. 8. Influence of velocity ratio on penetration resistance ratio, near-saturated fat clay (from reference 4)

ABSCISSA AXIS: AN IDEAL FLUID (HAS ZERO VISCOSITY)

ORDINATE AXIS. AN ELASTIC SOLID

CURVE A   A NEWTONIAN FLUID

CURVE B   A PSEUDOPLASTIC FLUID

CURVE C: A DILATANT FLUID

CURVE D: A BINGHAM PLASTIC

CURVE E: A PSEUDOPLASTIC MATERIAL WITH A YIELD VALUE, ψ

CURVE F: A DILATANT MATERIAL WITH A YIELD VALUE, ψ

NOTE: THE SLOPES OF THE DOTTED LINES REPRESENT THE APPARENT VISCOSITIES CORRESPONDING TO POINT b ON CURVE B, c ON CURVE C, e ON CURVE E, AND f ON CURVE F.

a.   Flow curves for various ideal rheological bodies (from reference 9)

CURVE DEPARTS FROM POWER-FUNCTION SHAPE AND TAKES NEAR-CONSTANT y-AXIS VALUE AT x-AXIS VALUE CORRESPONDING TO THRESHOLD VELOCITY FOR THE PARTICULAR COMBINATION OF CONE SIZE AND TYPE OF FINE-GRAINED SOIL
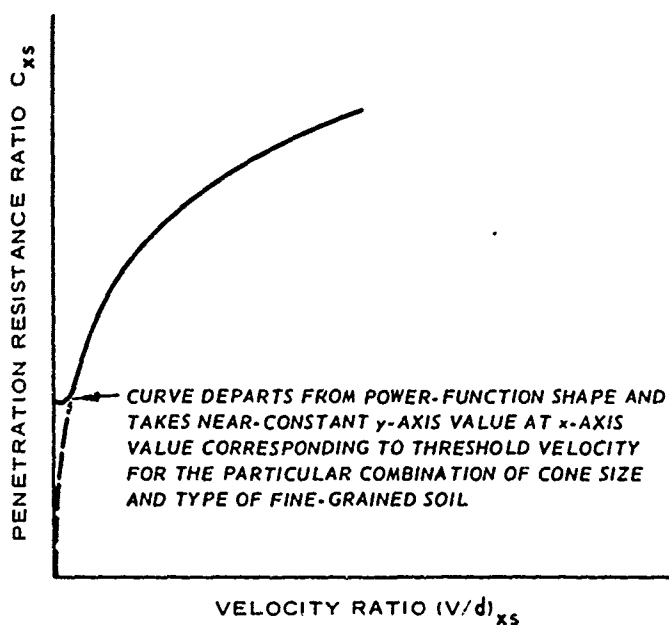
b.   Representative viscous-type flow curve for a cone penetrating a near-saturated, fine-grained soil

Fig. 9.   Flow curves

22

whose shearing stress versus rate of shear relation is nonlinear), and
for plastic materials (i.e. those for which $\psi > 0$), viscous behavior
can be described by an apparent coefficient of viscosity (slopes of
dotted lines in fig. 9a). This term represents the viscosity that a
Newtonian fluid would exhibit at the same given value of shearing stress
or rate of shear. For all but Newtonian fluids, however, the value of
this term changes as the point of interest changes. Thus, for plastic
materials and non-Newtonian fluids, a useful relation for describing
viscous flow is a plot of apparent coefficient of viscosity y/x (where
y is shearing stress and x is rate of shear) versus rate of shear
x. The general form of the equation for curve E in fig. 9a is

$$y - \psi = kx^n$$

where

ψ = yield stress = intercept on y-axis (arithmetic plot)

k = constant of proportionality; [i.e. the value of $y - \psi$,
when $x = 1.0$ on a plot of $\log (y - \psi)$ versus $\log x$]

n = slope of the line on a logarithmic plot

From this

$$\frac{y - \psi}{x} = \frac{kx^n}{x} = kx^{n-1} \tag{1}$$

For pseudoplastic materials, n in equation 1 varies between 0 and 1,
so that values of $n - 1$ must vary between -1 and 0.

31. In reference 4, $C_{xs}/(V/d)_{xs}$, a term that corresponds to
normalized y/x, was used instead of normalized $(y - \psi)/x$ in a log-
arithmic relation analagous to apparent coefficient of viscosity versus
rate of shear (fig. 10). The fact that this treatment, which apparently
ignores ψ, produces a good log-linear fit to the data over a wide
range of shear rates indicates that over this range the material may be
represented as a non-Newtonian fluid, without a measurable yield
strength. On the basis of earlier observations on threshold velocities,
shear stress at very low shear rates may be taken as a constant for a

23
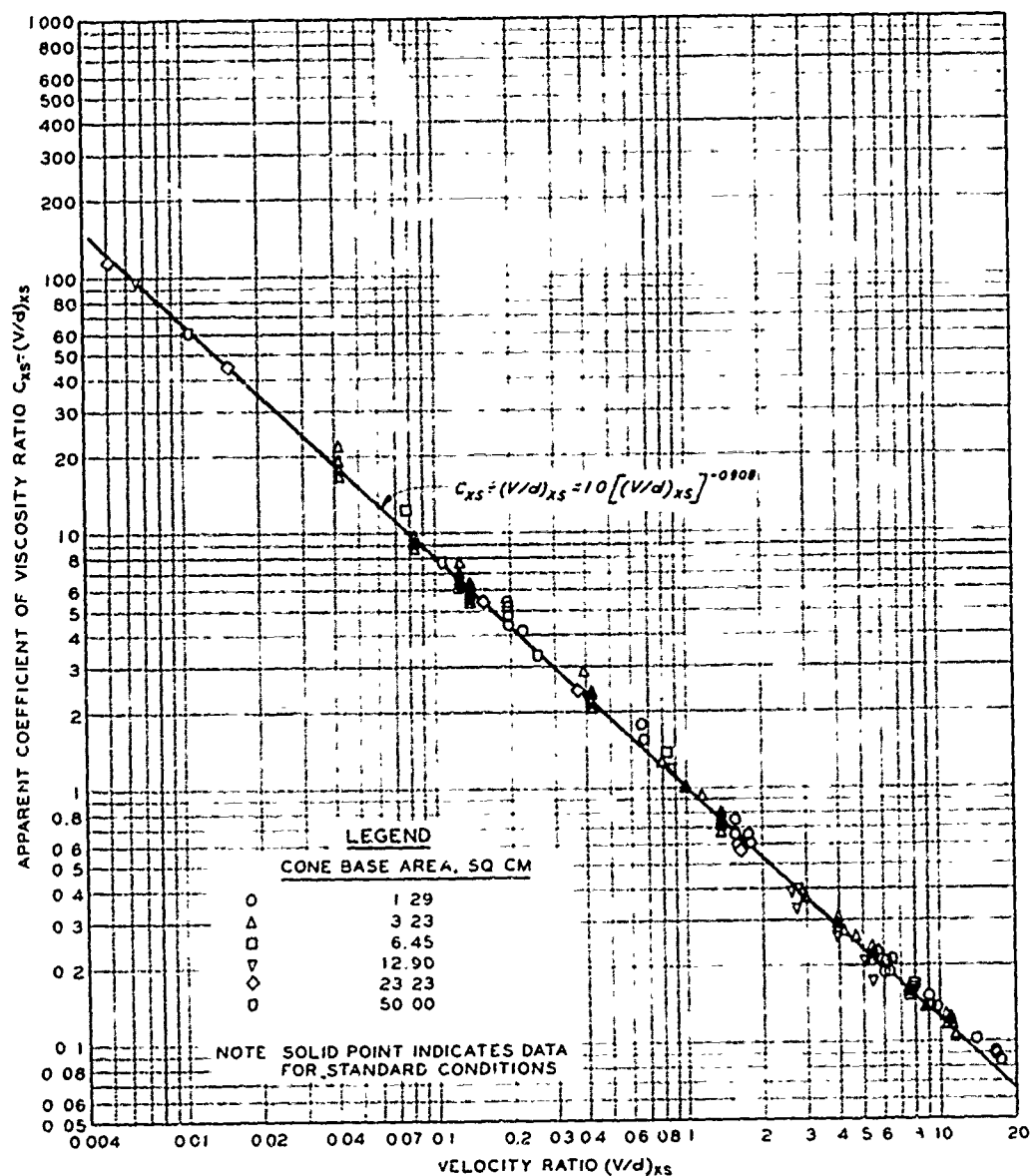
Fig. 10. Relation of apparent coefficient of viscosity ratio
to velocity ratio, near-saturated fat clay (from reference 4)

24

given combination of soil type and probe size and shape, leading to the representation in fig. 9b. The curve in fig. 9b differs from curve E in fig. 9a on two counts: (a) the dashed line in fig. 9b signifies that for velocity ratio values larger than defined by threshold velocities, the penetration resistance ratio versus velocity ratio relation can be described by a logarithmic relation passing through the origin, and (b) the value of the y-axis intercept is maintained near-constant over a measurable range of x-axis values, unlike the yield value in fig. 9a.

32. Other researchers have concluded that a logarithmic representation for pseudoplastic materials is adequate only within a still more limited range of values of rate of shear.[9] In particular, some suggest that the logarithmic function relating shearing stress to rate of shear for pseudoplastic materials fits only that part of the curve lying between two limiting straight-line portions (fig. 11). A literature
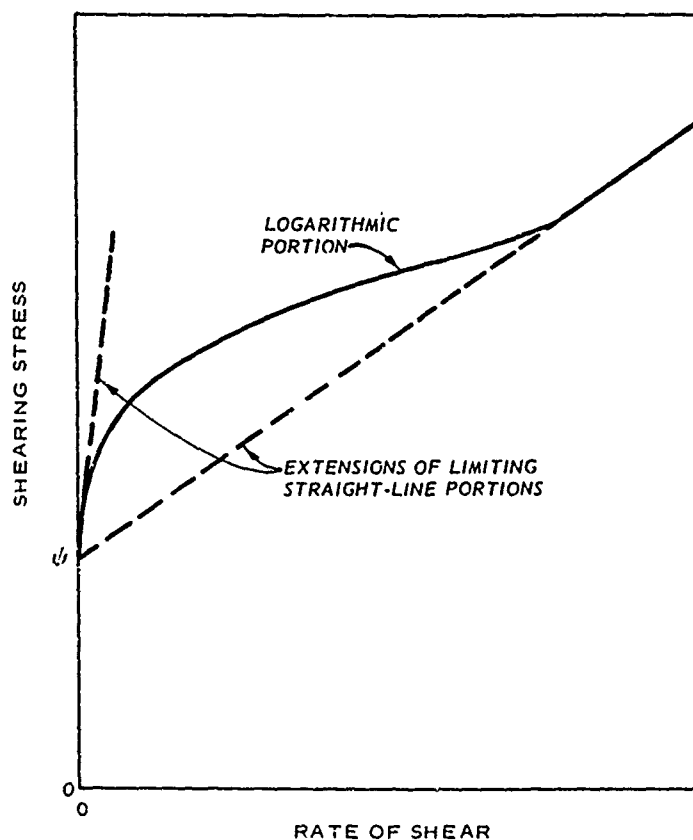
Fig. 11. Approximation of the flow curve of a pseudoplastic material with yield value (from reference 9)

25

search disclosed little data to define the shape of pseudoplastic ma-

terial flow curves at shear rates beyond the logarithmic portion. The

author of this report suggests that the increase in resistance of sat-

saturated, fine-grained soils with increasing probe penetration vel city

results from a combination of viscous and inertial forces, and tha this

increase can be described in a manner essentially the same as that e-

veloped in fluid mechanics for drag produced by bodies penetrating

broad variety of fluids, without limiting the scope of the logarit dc

representation of soil viscous behavior. (In this context, "drag" nd

"penetration resistance" are synonymous.) This suggestion is expl ed

further in paragraphs 42-62.

Influence of Probe Shape on Viscous Contributions
to Penetration Resistance

Flat plates

33. _Rectangular-base-area plates._ To establish a frame of fer-

ence, the data from tests in fat clay are examined first, and the i-

fluence of probe shape upon the fat clay results is delineated. T test

data are detailed in table 1. The starting point in analyzing the at

clay data was to apply a relation of the same type used in referer h

to describe the effects of velocity, size, and shape of probes on e

penetration resistance of saturated, fine-grained soils, i.e. to d er-

mine the utility of a relation of the type $P_{xs} = q(V/d)^n_{xs}$ (para-

graph 29). For circular-base-area plates, it was established in fer-

ence 4 that diameter d is appropriate for use as the linear dime ion

in $P_{xs} = q(V/d)^n_{xs}$. One item of particular interest in this anal is

was whether rectangular probes of different width-to-length ratios le-

velop different soil penetration resistance values, other conditi be-

ing equal (i.e. same probe base area and penetration velocity in given

soil). To ascertain this, ℓ $(=\sqrt{A})$ was substituted for d in t ve-

locity ratio, i.e. $(V/\ell)_{xs}$, so that a linear term of the same va

would be used for probes of the same size, but different base are

shape. (ℓ_x is the square root of the base area of any flat plate and

ℓ_s is the square root of the base area of the standard cone.) In

26

plate 1 the test data for rectangular flat plates in fat clay are plotted in the form of penetration resistance ratio, P_{xs} , versus velocity ratio, $(V/\ell)_{xs}$. To examine possible trends more closely, separate plots are given for the four length/width ratios examined. Plate 1 shows that using ℓ_x and ℓ_s , the equation

$$P_{xs} = 0.80 \left(\frac{V}{\ell}\right)_{xs}^{0.100} \tag{2}$$

describes the logarithmic relation of plate penetration resistance ratio to velocity ratio for probes with width-to-length ratios from 1:1 to 1:8 penetrating fat clay. Probe base areas in plate 1 range from 1.61 to 58.1 cm^2, penetration velocities from 5.82 to 1103 cm/sec, and soil strengths (C_s) from 164 to 899 kPa.

34. The closed symobls in plate 1 represent data from the soil car test section of high-strength fat clay, which had an average standard penetration resistance value C_s of 809 kPa. Open symbols in plate 1 represent data from fat clay soil cars with average C_s values of 210 and 290 kPa. No separation by soil strength levels was noted in any relations based on the fat clay soil car data. Since viscous flow is generally thought of in connection only with materials of near-fluid consistency, it is interesting to note that the relation in plate 1 appears to be defined as well by data from the high-strength soil car (closed symbols) as by those from the low-strength cars (open symbols).

35. Consolidation of the data in plate 1 is more evident in plate 2, which presents the relation of the apparent coefficient of viscosity ratio to the velocity ratio. The relation in plate 2 differs from that in plate 1 in that its ordinate term is ordinate/abscissa of plate 1. The relation in plate 2 is described by

$$\frac{P_{xs}}{(V/\ell)_{xs}} = 0.80 \left(\frac{V}{\ell}\right)_{xs}^{-0.900} \tag{3}$$

which is merely a direct algebraic transformation of equation 2.

36. <u>Circular-base-area plates.</u> Plate 3 presents the penetration data for circular-base-area flat plates in fat clay (table 1), plotted

in terms of the same variables used above. It shows that the same log-arithmic relations developed for rectangular plates hold true for circu-lar plates. The base areas of the circular plates range from 1.29 to 58.1 cm^2, and penetration velocities range from 5.82 to 1094 cm/sec. No systematic separation of the data by probe size or by soil strength is noted. Again, data from the high-strength soil car (closed symbols) clearly follow the common relation.

Cones

37. Data from penetration tests of 30-deg-apex-angle, right cir-cular cones in fat clay are plotted in plate 4. Relations correspond closely to those developed in plates 1-3 for the rectangular and circular-base-area plates. In plate 4a, the relation of cone penetration re-sistance ratio to velocity ratio can be described, despite an appreciable amount of data scatter, by

$$C_{xs} = 1.00 \left(\frac{V}{\ell}\right)_{xs}^{0.100} \tag{4}$$

In plate 4b, the relation of apparent coefficient of viscosity ratio to velocity ratio is described by

$$\frac{C_{xs}}{(V/\ell)_{xs}} = 1.00 \left(\frac{V}{\ell}\right)_{xs}^{-0.900} \tag{5}$$

38. The relations in plates 4a and 4b are in effect identical with those from the earlier study[4] shown in figs. 8 and 10, except for different ranges of the abscissa term and small differences in the ex-ponents of $(V/d)_{xs}$ or $(V/\ell)_{xs}$* for the two sets of ta. These

---

* $(V/\ell)_{xs} = (V/\ell)_x \Big/ (V/\ell)_s = (V_x/V_s)(\ell_s/\ell_x)$

$(V/d)_{xs} = (V/d)_x \Big/ (V/d)_s = (V_x/V_s)(d_s/d_x)$

For probes with a circular base area, such as the cones under consideration,

$$(\ell_s/\ell_x) = 0.886 d_s / 0.886 d_x = d_s/d_x$$

so that

$$(V/\ell)_{xs} \equiv (V/d)_{xs}$$

28

differences would, in fact, be barely perceptible if the new relations from plates 4a and 4b were redrawn upon figs. 8 and 10, respectively.

Influence of Soil Type on Viscous Contribution to Penetration Resistance

39. To investigate whether the mechanism of soil resistance to high-speed penetration changes as a function of soil type for near-saturated, fine-grained soils, tests were conducted in three soil types in this study--a fat clay, a lean clay, and a silt. Data from penetration tests in lean clay (table 2) are shown in plate 5 for flat plates and in plate 6 for cones. The relations in plate 5 are described by equations 2 and 3, and those in plate 6 by equations 4 and 5, all of which were used earlier to describe corresponding relations for the fat clay test results. Plates 7 and 8 present data from penetration tests in silt (table 3) with flat plates and cones, respectively. The relations for plates in the silt are described by

$$P_{xs} = 0.95 \left(\frac{V}{\ell}\right)_{xs}^{0.100} \tag{6}$$

and

$$\frac{P_{xs}}{(V/\ell)_{xs}} = 0.95 \left(\frac{V}{\ell}\right)_{xs}^{-0.900} \tag{7}$$

(plate 7); and for cones in the silt by

$$C_{xs} = 1.00 \left(\frac{V}{\ell}\right)_{xs}^{0.080} \tag{8}$$

and

$$\frac{C_{xs}}{(V/\ell)_{xs}} = 1.00 \left(\frac{V}{\ell}\right)_{xs}^{-0.920} \tag{9}$$

(plate 8).

40. In the relations for flat plates in equations 2 and 6, the

exponent n is 0.100 for all three test soils, but the coefficient is
0.80 for both fat and lean clays and 0.95 for the silt. For cones
(equations 4 and 8), the coefficient is 1.00 for all three soils, but
the exponent n is 0.100 for both clays, and 0.080 for silt. For all
three soils, the test data were sampled only when penetration resist.nce
and velocity values were stable (paragraphs 20 and 21). Also scatter of
the silt test data is not excessive (plates 7 and 8), so test controls
are thought not to be the reason for differences in corresponding equa-
tions for the silt and the two clays. Rather, these differences are
considered to result because, under shear deformation, the silt exhib-
ited compressive characteristics markedly different from those of the
clays. The soil surface depressed far more noticeably around probe pen-
etrations in the silt than in the clays, and depth to uniform per 'ra-
cion resistance values varied more for the silt than for the clays
(paragraph 20). Also, the silt (but not the clays) showed a pronounced
tendency under stress to bleed (i.e. to allow water migration to the
surface) and to move as a single mass. These observations suggest that
the stress-deformation mechanism of the silt was different from that of
the two clays, which is entirely reasonable.

41. In view of the fundamental differences in the physical behav-
ior of the silt and the clays as noted above, it is somewhat surprising
that differences between equations that describe their resistance to
high-speed plate and cone penetrations are as small as they are. One
possible reason for this is that for near-saturated, fine-grained soils,
the pattern of increase in penetration resistance caused by increasing
velocity is controlled primarily by speed-of-deformation effects which
take place largely within the water portion of the soil-water-air mix.
For two or more nearly saturated soils, then, quite large differences in
soil particle characteristics would be required before resistance-to-
deformation characteristics of the overall mixes became markedly differ-
ent. For most near-saturated, fine-grained clays, equations 2 and 4 are
considered adequate for describing viscous soil resistance to penetra-
tion by flat plates and cones, respectively. For near-saturated silts,
equations 6 and 8 likely are better.

30

Contributions of Viscosity and Inertia to Total
Soil Penetration Resistance

42. To this point, increases in the penetration resistance of
highly saturated, fine-grained soils caused by increasing the velocity
of the penetrating probe have been attributed entirely to the effects of
viscosity. In the following paragraphs, data for extremely large veloc-
ity ratio values developed at WES, together with data from high-speed
plate lift tests conducted at Battelle Institute, Frankfurt, Germany,[10]*
are analyzed in conjunction with relations discussed in paragraphs 33-40
of this report to begin an examination of the combined influence of vis-
cosity and inertia on soil penetration resistance.

WES high-velocity-ratio tests

43. In the earlier study[4] discussed in paragraphs 28-31, analysis
of data from five _horizontal_ penetration tests with cones in 8.2-m-long
soil cars of fat clay very similar to that used in this study suggested
that total soil penetration resistance (drag) measured at the higher ve-
locities in that study (maximum velocity, 451 cm/sec) was influenced not
only by viscosity, but also by some inertia. Those relations were ob-
scured by a significant amount of data scatter, and it was hoped that
the higher penetration velocities and the more elaborate controls of
soil strength in the tests reported herein would allow better definition
of the effects of inertia on soil penetration resistance.

44. Despite a fivefold increase in the maximum value of velocity
ratio (623 versus 120) for data examined thus far in the present study
as compared with that in the earlier one, it has still appeared that all
changes in observed soil penetration resistance were related solely to
viscous effects. A limited series of tests was conducted to increase
the range in velocity ratio even further (to 1134); results are plotted
in plate 9. To conduct these special tests within the constraints of
available apparatus, they were run in one mold of each of the three

---

* Data furnished in personal communication from Dr. Dieter Schuring,
  Cornell Aeronautical Laboratory, Buffalo, N. Y., 7 Jun 1972.

soils at velocities to more than 1000 cm/sec with a cone of very small diameter, 0.641 cm. Because only a 2.22-kN-capacity load cell was available to record penetration resistance at velocities greater than 300 cm/sec, the test molds were built to very large values of standard cone penetration resistance, so that measurable values of force would be produced. Even in these very dense test sections (C_s values of 1053, 1315, and 963 kPa for fat clay, lean clay, and silt, respectively), the forces generated by penetrating with the extrem / small cone (base area = 0.323 cm^2) were quite small (largest = 0.0955 kN) compared with the capacity of the load cell (2.22 kN). This, combined with the fact that the smaller the probe, the more sensitive it is to minor soil strength irregularities, made it not surprising that fairly substantial scatter should result in penetration resistance measurements obtained.

45. The logarithmic relation of apparent coeffi ient of viscosity ratio to velocity ratio is presented in plate 9a for tests made with the 0.323-cm^2 cone in the three test soils. The most important result in plate 9a is that essentially all of the observed change in soil penetration resistance is described in terms of viscous effects. It is important, too, to keep sight of the amount of change in the value of cone penetration resistance ratio caused by increasing the value of the velo ity ratio to well over 1000. The arithmetic plot in plate 9b illustrates that the relation given by equation 4 becomes very flat after velocity ratio values exceed about 50. Scatter of the test data is also more evident in plate 9b than in the logarithmic plot given in plate 9a. This scatter is not considered excessive when it is recognized that the largest difference between measured value of soil penetration r   ance force and that predicted by the curve for the data points in p   is 18.9 N, or less than 1 percent of the rated capacity of the loau ___ used. The change in shape of the curve of shear stress versus rate of hear hypothesi ! by some for very large values of rate of shear (paragraph 32 and fig. 11) is not suggested by the data in plate 9b.

Battelle Institute test results

46. During the early 1960's tests were conducted by the Battelle Institute (Frankfurt, Germany) to explore the possibility of generating

32

useful levels of vehicle support in very weak soils through the exploitation of soil inertial forces.[10] This work indicated that there ·s little practical potential for utilizing soil inertia for ground vehicle support. However, the data developed in that study, reexamined in the light of the present research, are useful in defining the domains of viscosity and inertia in vehicle-soil dynamics systems.

47. Description of tests. In the Battelle tests, a soil of "fluid mud" and "less fluid mud" consistencies, having cohesion (C) values of 1.4-1.9 kPa and 7.8 kPa, respectively,* was penetrated horizontally at velocities up to 27 m/sec by single rectangular plates, flat and with curvature along the chord length, of 2:1 aspect ratio** and areas of 24.5 and 98.0 cm^2. Grain-size distribution of the Battelle soil was not unlike that of the silt used in the study reported herein (compare figs. 1 and 12). The soil was contained in a circular soil bin (fig. 13) that was 41 cm wide, 41 cm deep, and 4.9 m in diameter. Tests were conducted by accelerating a test plate outside the soil until the desired speed was reached; suddenly immersing the plate in soil so that its upper, leading edge was level with the undisturbed soil surface; conducting the test in one revolution; and then slowly braking the plate until it stopped. Three angles of inclination (α) of the plate to the forward horizontal were tested at Battelle--15, 30, and 60 deg. The primary test response measured was plate lift, i.e. the vertical component of total force imparted to the plate by the soil. Test results are presented in table 4.

48. Considerations from fluid mechanics. Before examining the Battelle results, it is useful first to consider a technique commonly employed to describe the lift force F_L acting on a completely submerged body penetrating through any one of a broad variety of homogeneous fluids. From fluid mechanics,

---

* Measured under near-static conditions with a "simple, self-fabricated shear box."
** Width/chord length measured in the direction of travel.
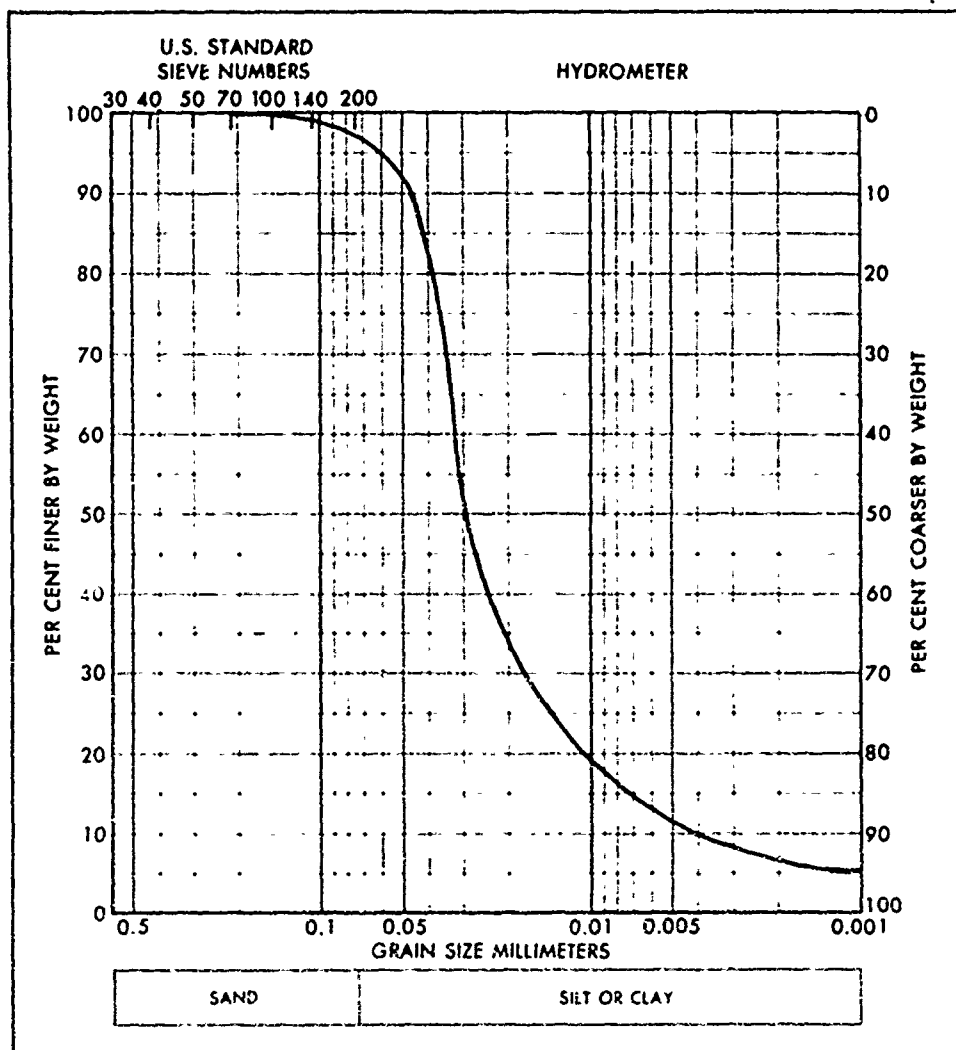
Fig. 12. Gradation of Battelle Institute test soil

$$F_L = \frac{C_L \rho A V_x^2}{2} \qquad (10)$$

where

C_L = dimensionless total lift coefficient

ρ = density of the fluid (mass per unit volume)

A = area of the body

V_x = velocity of the penetrating body relative to that of the surrounding fluid (in the direction of penetration)

34
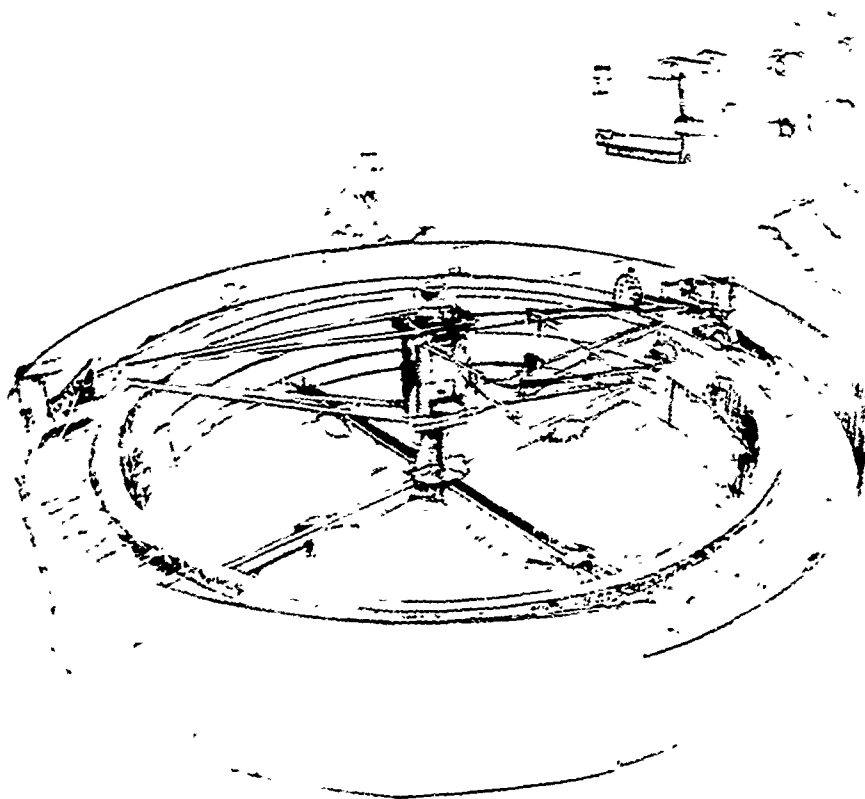
... ... of Battelle Institute circular ... ...
... manometer system. from reference 1.

... summary of ... penetrated by bodies at subsonic speeds, ...
... ... a function of two variables, the geometry of ... ...
... body and reynolds number R_p. Reynolds number represents the
ratio of characteristic inertial forces F_i to characteristic viscous
forces ..., acting on a body, and is expressed by

$$ R_R = \frac{F_i}{F_v} = \frac{L^2 V_x^2 \rho}{L V_x \eta} = L V_x \frac{\rho}{\eta} \tag{1} $$

where

L – a characteristic linear dimension of the penetrating body

35

η = coefficient of viscosity of the fluid*

V_x and ρ are defined above.

Relations among C_L , body shape, and N_R were developed by means of dimensional analysis. One major result of this analysis is that immersed bodies of the same shape and alignment with the flow (i.e. models of each other) penetrating homogeneous fluids at subsonic speeds possess the same lift coefficient if their Reynolds numbers are the same.

50. In a logarithmic plot of C_L versus N_R , the curve for a particular system (material density and body geometry fixed) can be divided into three ranges--a viscous range (viscous effects acting, inertial effects insignificant), a transition range (sizable viscous and inertial effects acting), and a dynamic range (inertial effects dominant). The shape of the C_L versus N_R curve has long been established in fluid mechanics for a plate immersed in air or water, as illustrated in fig. 14 for a particular case. In the viscous range, the slope of
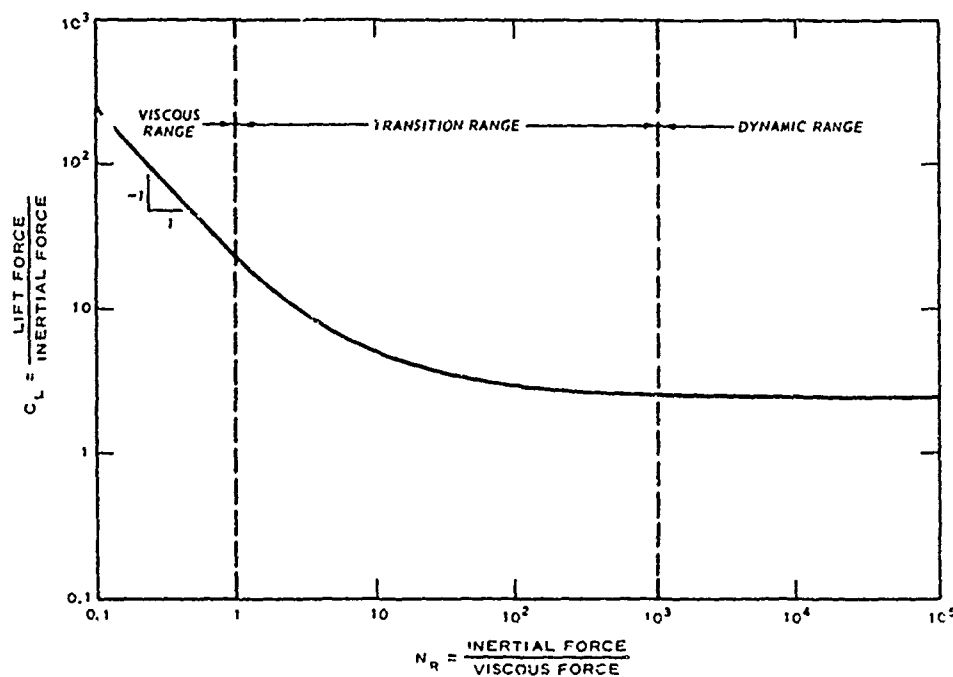
Fig. 14. Representative lift coefficient versus Reynolds number curve

---

* η is also known as "viscosity," "absolute viscosity," and "dynamic viscosity" of a fluid. In the case of a pseudoplastic fluid, the prefix "apparent" should be placed before each of these names.

the curve is -45 deg, i.e. negative 1:1, indicating that $C_L \alpha N_R^{-1}$ [(lift/ inertial forces) α(inertial forces/viscous forces)$^{-1}$] or lift is directly proportional to viscous forces. In the dynamic range, the curve is practically flat, so (lift/inertial forces) = a constant, i.e. lift is directly proportional to inertial forces only. The shape of the curve in the transition range depends on both the viscous and the inertial .properties of the fluid.

51. <u>Interpretation of Battelle test results.</u> Data from the Battelle tests are presented in plate 10 in a dimensionless logarithmic plot of lift coefficient $C_L = F_L / \left[\left(\rho A V_x^2 \right) / 2 \right]$ versus plate-soil numeric $\pi_s = \left[\left(\rho A V_x^2 \right) / 2 \right] / CA$. Discussion of the Battelle results will center first on interpretation of the relation in plate 10, and then on possible alterations to this relation to make it more generally applicable.

52. The format in plate 10 closely matches the one used in reference 10, and the curves in plate 10 have the same general shape as the one in fig. 14 (with the transition range in plate 10 depicted as lying between π_s values of about 1.5 and 150). Data in plate 10 separate, however, by level of soil cohesion C and, for values of π_s larger than about 1.5, by inclination angle α . Only five data points are shown in plate 10 for the smaller (3.5- by 7-cm) plate (all with $\alpha = 15$ deg), and only one of them has a π_s value substantially less than 150 [coordinates (23.0,0.412)]. The π_s value of this one point is more than two times larger than the curve for $\alpha = 15$ deg , so no firm conclusion can be drawn regarding whether the C_L versus π_s relation is independent of plate size below the inertial range. Data for the 3.5- by 7-cm plate intermingle with those of the 7- by 14-cm plate, $\alpha = 15$ deg , for π_s values of about 150 and larger, indicating that the C_L versus π_s relation may be independent of size in the inertial range.

53. An important consideration in plate 10 is that the curve departs from the straight-line configuration at π_s values larger than only about 1.5. For $C = 1.7$ kPa and $\rho = 1.9$ kN-sec^2/m^4 (approximate conditions of the open-symbol data in plate 10), penetration velocity is 1.64 m/sec at an inertial force ratio of 1.5. Thus, inertial forces can be brought into play at relatively small values of penetration velocity.

37

This emphasizes the point that it is the _ratio_ of inertial to cohesion forces in π_s that makes possible a curve shape like that in plate 10, not penetration velocity per se or probe size at all, since probe base area A cancels in π_s . This also indicates that the weakest consistency of the WES test soils was several times stronger than that of the Battelle soil, since no inertial effects were observed in the WES penetration tests, even at velocities to more than six times greater than 1.64 m/sec.

54. The relation of lift force to velocity, which is somewhat obscure in plate 10, is shown in fig. 15a for the 7- by 14-cm and 3.5- by 7-cm plates, $\alpha = 15$ deg , $C = 1.4$-1.9 kPa . These data are adequately described by the equation

$$F_L = a + bV_x^2 \tag{12}$$

where $a = k_1 A$ and $b = k_2 A$, i.e. values of intercept a and coefficient b each increase directly with plate base area A . This relation is true only for different plates penetrating a soil or soils of the same density ρ , since the inertial component of lift force is defined as

$$F_i = \frac{C_i \rho A V_x^2}{2} \tag{13}$$

where C_i is dimensionless inertial lift coefficient.

55. In fig. 15b, the same data as in fig. 15a are described by the equation

$$\frac{F_L}{A} = k_1 + k_2 V_x^2 \tag{14}$$

(i.e. by the equation that results from dividing each term in equation 12 by A). The relations in figs. 15a and 15b demonstrate that, for plates of different sizes, separate equations must be used to describe lift _force_ as a function of velocity, but a single equation is adequate to describe lift _stress._ Equations 2 and 6, found adequate for
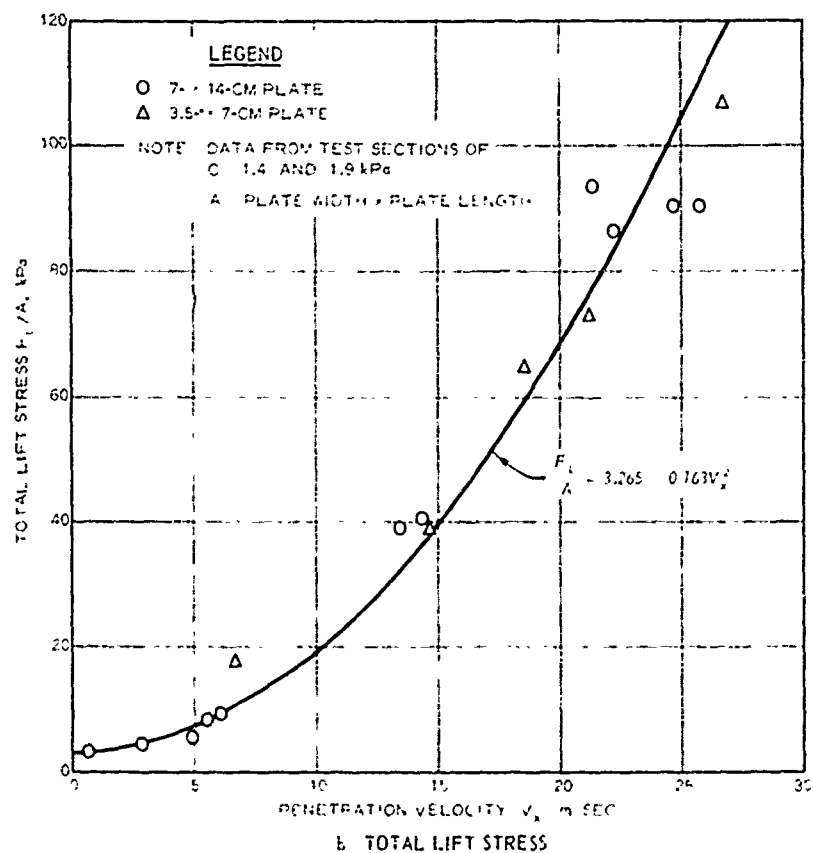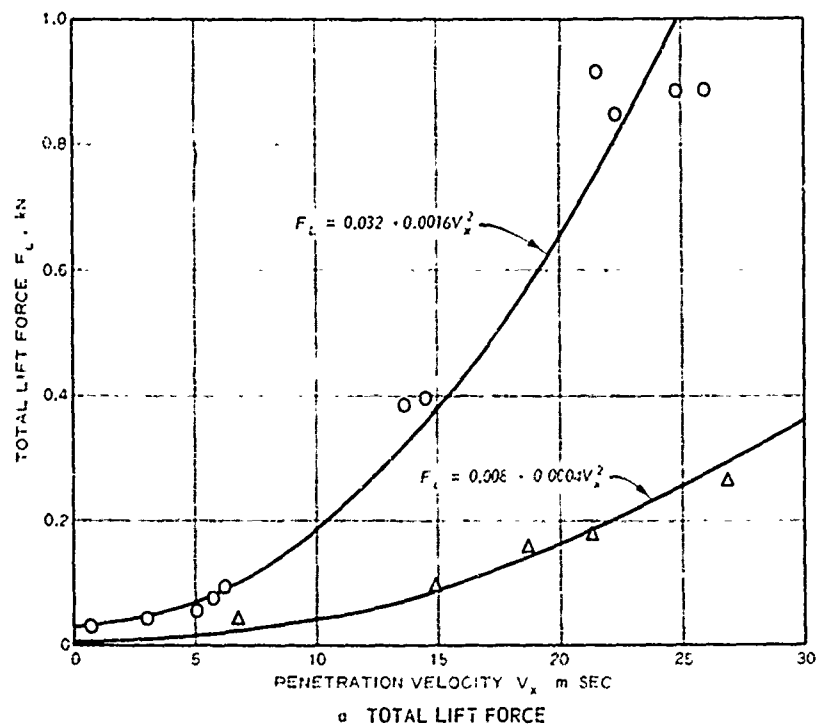
Fig. 15. Relations of total lift force and total lift stress to
penetration velocity for model-prototype plates in fluid mud

describing penetration resistance for many flat probe sizes and shap s
in saturated clays and silts, respectively, would separate into any re-
lations of the form

$$F = P_x A_x$$

if force instead of stress on various probes were taken as the v riable
of interest. The point is that unifying relations that describe either
the effects of soil viscous behavior on penetration resistance o iner-
tial effects on soil lift do so by considering stress (force per unit
area) on the probe, not force. Note that the variables in plate 10
could just as well be expressed as $(F_L/A)/\left[(\rho V_x^2)/2\right]$ versus
$\left[(\rho V_x^2)/2\right]/C$, two ratios of stresses. Thus, separation of the d ta in
plate 10 is not explained on the basis that the variables consid red re-
flect forces and not stresses. (Reasons for this separation are dis-
cussed in paragraphs 59-61.)

56. It is of interest to note that the curve shape antici ated by
some researchers for pseudoplastic materials at large values of at of
shear (fig. 11) is not realized when soil penetration resistance stress
is dominated by viscous effects (plate 9b, for example) or when oil
lift stress is dominated by inertial effects (fig. 15b, for exam le).
A situation might be envisioned where viscous and inertial force com-
bine to produce a near-linear curve shape for a saturated soil w t in a
limited range of values of penetration velocity. (Such an occur en e
would have to take place in the transition range.) It does not eem
possible, however, that the shear stress versus rate of shear re ation
for saturated, fine-grained soils would follow a straight-line p t ern
for an extended range of arge values of rate of shear.

57. Relation to soil-vehicle systems. Inertial force i
plate 10 for the open-symbol data become dominant at plate-soil umeri
$\pi_s = 150$; for $C = 1.7$ kPa and $\rho = 1.9$ kN-sec^2/m^4 , velocity V_x
this point is 16.4 m/sec (59 km/hr). The data in plate 0 also
that curves for a single inclination angle α , but different v ue
C , may be parallel throughout the range of values of π . I hi

40

true, then the velocity V_x to reach an inertia-dominated lift force condition increases directly with cohesion C. For $C = 17$ kPa and $\rho = 2.2$ kN-sec^2/m^4, V_x at $\pi_s = 150$ would be 48.1 m/sec (173 km/hr).

58. Data are not available to define precisely the strengths of the "fluid mud" and "less fluid mud" of the Battelle tests in terms of a standard measurement (as opposed to cohesion C measured with a "self-fabricated shear box"--see paragraph 47). A study at WES of the relations between C_s and the cohesion of saturated clays as measured by several types of soil shear devices showed that C_s values were from 5.3 to 12.5 times larger than those of "cohesion," the magnitude of the multi-plier varying with the type of test device.[6] Using even $C_s = 12.5 \, C$, values of C_s for the examples in paragraph 57 are much too small to permit a conventional ground vehicle to attain velocities such that in-ertial effects dominate lift force $(V_x = 59$ km/hr at $C_s = 21$ kPa and $V_x = 173$ km/hr at $C_s = 213$ kPa). For some other applications, however (dynamic probe testing and, possibly, some aircraft landings and take-offs on earthen airstrips, for example), combinations of velocity and soil strength might well be encountered such that lift force is domi-nated by inertial forces.

59. <u>Alterations to the C_L versus π_s relation.</u> One means for consolidating data in the inertial range for the C_L versus π_s rela-tion in plate 10 is to substitute for base area A in the term $\left(\rho A V_x^2\right)/2$ the area A_x projected normal to the direction of penetration (i.e. $A_x = A \sin \alpha$). The success of this operation is demonstrated in plate 11, where, except for the encircled data points,* separation of the data by inclination angle α is effectively removed. Use of A_x in the C_L versus π_s relation does <u>not</u> cause it to match more closely the classic C_L versus N_R relation (fig. 14), because the characteristic area used

---

* The leftmost encircled data point is the one for the lowest-speed test of the 3.5- by 7-cm plate. In paragraph 52, this point was con-sidered not to verify independence of the C_L versus π_s relation on size outside the inertial range. Values of lift coefficient for the other two encircled data points are suspected to have been measured too small by a factor of two.

in the latter relation is projected area normal to the lift vector,[11] i.e. $A \cos \alpha$ for the case at hand.

60. This difference between the C_L versus π_s and the C_L versus N_R relations raises the basic question of whether even a modified C_L versus π_s relation should be expected to describe results of the Battelle tests at the soil surface in a manner corresponding to the C_L versus N_R relation for probes completely submerged in fluids. The primary difference between the two systems is the presence of a free surface (i.e. the soil-air surface) in the Battelle tests. Any effect of this surface on lift force would be expected to emerge primarily in terms of gravity (or weight) forces acting on the plate. Schuring[10] correctly notes from a relation similar to that in plate 10 that the inclination angles of the plates did not affect lift force in the range of π_s values less than about 1.5, although a plate inclined at 15 deg lifts much less soil weight than a plate at 60 deg. Thus, weight force is unimportant and can rightly be neglected.*

61. The remaining important consideration in comparing the C_L versus π_s and the C_L versus N_R relations centers on the denominators of π_s and N_R (see plate 11 and fig. 14, respectively). CA in the denominator of π_s represents a system force associated with an essentially static measure of soil shear strength, C . From equation 11, characteristic viscous force F_v in the denominator of N_R can be expressed as $F_v = LV_x \eta = A(V_x/L)\eta$; i.e. F_v is a shear force acting on an area A that reflects the action of a velocity gradient (or rate of shear), V_x/L , and a measure of viscosity, η . Substituting for C in π_s a soil strength term that reflects the viscous behavior of soil would make the correspondence of π_s to N_R very close, and presumably would make the method of presentation in plate 11 more general. This suggests substituting for C a measure of soil penetration resistance stress similar to P_x from the WES vertical penetration tests (see equations 2 and 6). Unfortunately, this step is not possible

---

* The relation in plate 11 also suggests that weight force can be neglected, since the effect of α on the C_L versus π_s relation is effectively eliminated for the full range of data in that plate.

at present because (a) data are not available to define with an accept-
able degree of assurance the C_s values of the Battelle test soil, and
(b) major differences between WES and Battelle test systems examined in
this report disallow making a direct substitution. (In WES tests, the
resisting force parallel to the direction of penetration was measured as
the probe moved vertically within the soil mass; in the Battelle tests
the force perpendicular to the direction of penetration was measured as
the probe moved horizontally at the soil surface.)

Summary

62. Information described herein from examination of the Battelle
test results can be summarized as follows: (a) Insight was gained into
the behavior of lift force F_L developed by plates moving at the soil
surface by examining the C_L versus π_s relation (paragraphs 51-56).
(b) At least tentative conclusions were drawn directly from this rela-
tion with respect to the influence of inertial forces on vehicle lift
support (paragraphs 57-58).* (c) The C_L versus π_s relation bears
some resemblance to the classic C_L versus N_R relation (described in
paragraphs 48-50). It was possible to eliminate data separation by in-
clination angle α for the C_L versus π_s relation (paragraph 59),
but data are not available at present to demonstrate independence of
this relation on plate size except within the inertial range of opera-
tion (paragraph 52), or to eliminate separation of this relation accord-
ing to soil strength (paragraph 61). These last two considerations
should receive attention in future research efforts.

---

* An equation of a form very similar to equation 4 has been used suc-
cessfully to describe sizeable changes in soil strength attributable
to viscosity that were caused by a range of wheel translational veloc-
ities routinely developed by ground vehicles in the field.[3]

PART IV: CONCLUSIONS AND RECOMMENDATIONS

Conclusions

63. Based on the analysis of the test results reported herein, the following conclusions are drawn:

    a. The penetration resistance of fine-grained soils saturated to at least 90 percent is significantly affected by changes in penetration velocity and probe size, but very little by the shape of the base of the probe (at least for flat-base-area probes) (paragraphs 28-38).

    b. Over the range of conditions where penetration resistance increases with velocity, the viscous behavior of the three fine-grained WES test soils is closely related to that of a classic rheological material, a pseudoplastic fluid (paragraphs 28-32). For cones and plates in near-saturated clays, the logarithmic equations that describe these relations are $C_{xs} = 1.00(V/\ell)_{xs}^{0.100}$ and $P_{xs} = 0.80(V/\ell)_{xs}^{0.100}$, respectively. For a near-saturated silt, $C_{xs} = 1.00(V/\ell)_{xs}^{0.080}$ and $P_{xs} = 0.95(V/\ell)_{xs}^{0.100}$ appear better for the cones and plates, respectively (paragraphs 33-41).

    c. No noticeable inertial effects were produced in the WES probe tests, although velocities to 1221 cm/sec and $(V/\ell)_{xs}$ values to 1134 were developed (paragraphs 43-45).

    d. Inertial effects strongly influenced soil lift force in horizontal plate penetration tests conducted at the Battelle Institute, Frankfurt, Germany. These effects can be described by a dimensionless lift coefficient C_L versus plate-soil numeric π_s relation that is similar to the C_L versus N_R (Reynolds number) relation used in fluid mechanics for this purpose (paragraphs 46-56).

    e. Tentative conclusions from the C_L versus π_s relation indicate that only for an extremely unusual set of

44

conditions--very low soil strength coupled with very high translational speed--will vehicle· be assisted significantly by inertial lift forces developed in the supporting soil (paragraphs 57-58). Routine vehicle speed-soil strength operating conditions can be influenced significantly by soil viscous phenomena, however (paragraph 62). A more likely situation wherein inertia influences soil strength significantly is that of dynamic probe testing of soils--air-dropped p····es, for example--and, possibly, some aircraft landings and takeoffs (paragraph 58).

f. Separation of the C_L versus π_s relation by plate inclination angle can be eliminated by using area A_x projected normal to the direction of penetration instead of plate base area A in the term $\left(\rho A_x V_x^2\right)/2$ that appears in both C_L and π_s (paragraph 59).

g. Data are not presently available to demonstrate conclusively whether the C_L versus π_s relation is fully independent of plate size (paragraph 52). It is suggested that separation of the C_L versus π_s relation by levels of soil strength can be eliminated by replacing soil cohesion C (in π_s) with a suitable measure of soil strength that reflects the viscous behavior of soil (paragraph 61).

Recommendations

64. Based on the experience gained in this study, it is recommended that:

a. Additional high-speed penetration tests be conducted in very weak, saturated, fine-grained soils to provide data that will resolve questions raised in g above.

b. A study of the patterns of soil flow around a penetrating element (whether probe, wheel, or other) be initiated to understand better the source of the viscous and inertial

45

components of overall soil penetration resistance.

c. A comprehensive study of the type reported herein be made of coarse-grained soils.

LITERATURE CITED

1. Department of the Army, "Soils Trafficability," Technical Bulletin ENG 37, Jul 1959, U. S. Government Printing Office, Washington, D. C.

2. Schreiner, B. G., "Mobility Exercise A (MEXA) Field Test Programs; Performance of MEXA and Three Military Vehicles in Soft Soil," Technical Report M-70-11, Report 2, Vol 1, Mar 1971, U. S. Army Engineer Waterways Experiment Station, CE, Vicksburg, Miss.

3. Turnage, G. W., "Performance of Soils Under Tire Loads; Application of Test Results to Tire Selection for Off-Road Vehicles," Technical Report No. 3-666, Report 8, Sep 1972, U. S. Army Engineer Waterways Experiment Station, CE, Vicksburg, Miss.

4. _____, "Measuring Soil Properties in Vehicle Mobility Research; Effects of Velocity, Size, and Shape of Probes on Penetration Resistance of Fine-Grained Soils," Technical Report No. 3-652, Report 3, Nov 1970, U. S. Army Engineer Waterways Experiment Station, CE, Vicksburg, Miss.

5. Freitag, D. R., "A Dimensional Analysis of the Performance of Pneumatic Tires on Soft Soils," Technical Report No. 3-688, Aug 1965, U. S. Army Engineer Waterways Experiment Station, CE, Vicksburg, Miss.

6. Smith, J. L., "Strength-Moisture-Density Relations of Fine-Grained Soils in Vehicle Mobility Research," Technical Report No. 3-639, Jan 1964, U. S. Army Engineer Waterways Experiment Station, CE, Vicksburg, Miss.

7. McRae, J. L., Powell, C. J., and Wismer, R. D., "Performance of Soils Under Tire Loads; Test Facilities and Techniques," Technical Report No. 3-666, Report 1, Jan 1965, U. S. Army Engineer Waterways Experiment Station, CE, Vicksburg, Miss.

8. Wismer, R. D. and Luth, H. J., "Rate Effects in Soil Cutting," Journal of Terramechanics, Vol 8, No. 3, 1972, pp 11-21.

9. Van Wazer, J. R. et al.. Viscosity and Flow Measurement; A Laboratory Handbook of Rheology, Interscience Publishers, New York, 1963, pp 12-19.

10. Schuring, D., "A Contribution to Soil Dynamics," Journal of Terramechanics, Vol 5, No. 1, 1968, pp 31-37.

11. Daugherty, R. L. and Ingersoll, A. C., Fluid Mechanics with Engineering Applications, McGraw-Hill, New York, 1954, pp 288-331.

Table 1

High-Speed Penetration Tests in the Tensile Properties of Various Tapes and Films

Test No.	Standard Penetration Resistance $x \times 6 \times$	Max Penetration Resistance Force[*] F_x	Average Penetration Resistance[**] x or F_x $(F/A_x \cdot x/a)$	Penetration Resistance Rat.[***] x_2 or F_{x_2}	Penetration Velocity V_x cm/sec	Velocity Rat. V_x x_2	Apparent with cent of Viscosity Rat.[**] V_{x_2} or $V \cdot x_2$ $: V/t \cdot x_2$

Table 1 Continued

Test No.	Standard penetration resistance c, ...	Soil penetration resistance ...	Average penetration resistance c_x or l_x	Penetration resistance ratio c_x ... l_x	Penetration velocity l_x ...	...	Apparent ... x ... l_x ...

... cm-dia, ... -base-Area, Flat Circular Plate

... (some-dia, ...-cm base-Area, Flat Circular Plate

...-cm-dia, ...-base-Area, Flat Circular Plate

... cm-dia, ... -base-Area, Flat Circular Plate

... uniform base-Area, Flat ... Plate

... cm, uniform base-Area, Flat ... Plate

... base-Area, Flat ... Plate

Table 1 (Concluded)

	Standard Penetration Resistance Force P_s, klb	Total Penetration Resistance Force P, N	Average Penetration Resistance σ_x or P_x (P/A_x), klb	Penetration Resistance Ratio σ_{xs} or P_{xs}	Penetration Velocity V_x cm/sec	Velocity $(V_x)_{xs}$	Apparent Coefficient of Viscosity μ_a or μ_x $(\sigma/V)_{xs}$

Table 1

High-Speed Penetration Tests in Sand, Clay with Probes of Various Types and Sizes

Test No.	Standard Penetration Resistance f_s, kPa	Area Penetration Resistance Force* F_x, N	Average Penetration resistance** $(F/A)_x$, kPa	Penetration Resistance Ratio** c_{xs} or F_{xs}	Penetration Velocity V_x cm/sec	Velocity Ratio $(V/v)_{xs}$	Apparent Coefficient of Viscosity Ratio** c_{xs} or F_{xu} : $(V/v)_{xu}$

1.13-cm-diam, 1.0-cm²-Base-Area Cone

Test No.							
.1-1-1-6			745	1.120		.30	.17
..-1-1-3				1.351		16.	
7.-1-1-4			1101	1.707	11.		
.9-1-1-5			115.	1.751	3.	1-1	
49-1-1-6	5.91		1341	1.969	1.9		
4.-1-1-7	350	197	1.7.	4.017	11.	97	

1.63-cm-diam, 2.73-cm²-Base-Area Cone

Test No.							
20-1-2-4	.15			1.817	10.		
16-1-2-4	215	45.0	.63	1.443	11.	3.	.3
4P-1-2-5	250	16.	514	1.096	339	112	1.
47-1-2-6	35.	.16	.06	1.057	1.37	3.	
45-1-2-7	353	.13	.57	1.607	1013	39	

2.05-cm-diam, 11.9-cm²-Base-Area Cone

Test No.							
17-1-3-6	142	100	157	1.17	11.9	1.	
19-1-3-4	159	.74	118	1.3.	113	17.	
14-1-3-9	100	.47	190	1.960	77	1.	.117

4.73-cm-diam, 15.8-cm²-Base-Area Cone

Test No.							
17-1-4-2	14.	407	176	1.112	10.	1.1	.4
19-1-4-4	193	550	213	1.348	109	1.	.1
12-1-4-6	121	559	28	1.984	9.	115	

.64-cm-diam, 0.323-cm²-Base-Area Cone

Test No.							
51-1-24-2	1315	44.0	1312	1.036	10.	10.	
51-1-24-4	1325	49.	28	1.673	107	13	.117
51-1-24-5	1315	74.6	4.07	1.	9.	97	
51-1-2-6	1315	5.1	350	1.7.		107	
51-1-24-7	1315	9.5	357	1.149	1.	113.	

1.28-cm-diam, 1.7-cm²-Base-Area, Flat Circular Plate

Test No.							
22-1-5-3	57.	97.	59	1.59	41.	17.	
47-1-5-4	5.5	113	57	1.77	12.	1.	
49-1-5-5	.91	22.	A.	1.544	9.5	1-1	. 45
49-1-5-6	.61	1.4	1117	1.5	17.	4.	. 31
4.-1-5-7	30.	1.					

1.9-cm-diam, 2.7-cm²-Base-Area, Flat Circular Plate

Test No.							
21-1-7-4	7.	1.9	29	1.	1.	.1	
1-1-7-4	4.	.9	73.	1.132	11	.	
57-1-7-5	710	7.	49	1.	7	11	.1
60-1-7-6	71.	35	75	1.52		17	
49-1-7-7	393	1.	5.	1.	11	17	

2.05-cm-diam, 1.0-cm²-Base-Area, Flat Circular Plate

Test No.							
8-1-8-2	.1	7	4	.5			.
10-1-8-4	5.	. 5	7	1.7		1.	.
49-1-8-6	7.4	4	5.	1.7	4	1.	.

4.73-cm-diam, 5.8-cm²-Base-Area, Flat Circular Plate

Test No.							
9-1-9-2	31.	7.	.7	1.	1.	1.3	.1
10-1-9-4	4.	7	7.7	3	1.	15.	.1
49-1-9-6	.	.	11	1.	.	1	.

1.7-cm-diam, 1.0-cm²-Base-Area, Flat Circular Plate

Test No.							
.5-1-11-2	1	7.	7	.	1.	.1	..
.5-1-11-4	.	1.	7	1	1.	1.	.
.5-1-11-5	.	.	.	1.	11.	7.	.
4.5-1-11-6	7	.	4	1.	.	15.	.
4.5-1-11-7	1.	1.7	7.	1.	7.	4.	.7
4.5-1-11-8	.	.	..	1.17	1.	..	.

(Continued)

* See paragraph ...
** For tests of sand, the terms that apply are c_{x}, c_{xs}, and V_{xs}, v_{xs}. For tests of clay, the terminology applicable are F_{x}, F_{xu}, and F_{x}, f_{xu}. See NOTATION, page ..., for definitions.

Table 7

Mild-Steel Penetration Tests in Silt at Penetrators of Various Shapes and Sizes

Test No.	Standard Penetration Resistance c_b, kPa	Soil Penetration Resistance Force* P, N	Average Penetration Resistance** c_x or P_x (P/A_x), kPa	Penetration Resistance Ratio** c_{xc} or P_{xc}	Test Plate Velocity v_x cm/sec		
	1.07-cm-diam, 1.03-cm²-Base-Area Cone						
24-1-1-.		7.2	133	0.78			
17-1-1-2	9	.3	9	1.04			3.
20-1-1-.	5	100		1.30	11.		7.
5-1-1-.	77	11.		1.59	71		
26-1-1-.	4	114		1.07	11.7		
	.02-cm-diam, 3.30-cm²-Base-Area Cone						
30-1-.-.	4	135	.17	1.06			3.
3 -1-.-.	4	14	440	1.073	11.		7.
64-1-.-.	1	231	715	1.273	.		
6 -1-.-.	.	37.	55.	1.49	11.1		
40-1-.-7	4	71	4.7	1.	11.1		
	.03-cm-diam, 10.3-cm²-Base-Area Cone						
3 -1-3-.	10	35	140	0.9.9	7.5		
4 -1-.-.	1	4.	11	.83	1		3.
54-1-3-.	137	314	343	1.77.	1		6.
	.73-cm-diam, .5.0-cm²-Base-Area Cone						
30-1-4-.	1	5	1	0.77	7.		3.
4 -1-4-.	133	7	1.	5.0.	1		
53-1-4-5	237	7.	5	1.4.	11		
	1.21-cm-diam, 4.3.2-cm²-Base-Area Cone						
-1-2-.	3	45.	1322	1.3.3	7	11	
5-1-.-.	3	.3.	1	1.46	1		
5-1-.-.	4	7.	1	1.7	.		
4-1-.-.	3	.7	1947	1.951			
5-1-.-7	3	7.	33	.7			
	1.07-cm-diam, 1.03-cm²-Base-Area, Flat Circular Plate						
3 -1-7-.	4	7.	13	1.51			
7-1-7-3	5	14.	1351	1.4		1	
7-1-.-.	4	134	10.	1.	117		
-1-7-.	7	1.	11.	1.7.			
-1-7-.	77	1.	1	.	1		
-1-7-.	71	1	1.7	.			
	.02-cm-diam, 3.30-cm²-Base-Area, Flat Circular Plate						
-1-7-.	.	1	.	1.	.	1	
-1-7-.	42	7	.	1.	.1.		
3-1-7-5	73	7.	11.7	1.	7		
-1-7-.	71	.	.	1.31.	11		
-1-7-.	7	17	.	1.3.7	17.		
	.03-cm-diam, 10.3-cm²-Base-Area, Flat Circular Plate						
-1-.-.	.	.	7.	1.	1		
-1-.-.	5	7	7.	1.173	1		
-1-.-.	107	1	17	1.	.		
	.73-cm-diam, .5.0-cm²-Base-Area, Flat Circular Plate						
3-1-.-.	.	114	2	1.3	11.		
3-1-.-.	.	1	3	1.3	1.		
	1.21-cm-diam, 4.3.2-cm²-Base-Area, Flat Circular Plate						
-1-11-.	.	77.	7	1.17	1.		
-1-11-3	.	1.	.	1.31	.		
-1-11-.	.	.	3	1.	11		
-1-11-.	.	171	1.	1.7	.		
-1-11-.	7	17	11.1	1.335	11.		
-1-11-7	5.1	1.	7	1.	1.1		

(Continued)

* See Footnote 17.
** For tests of cones the terms that apply are c_x, c_{xc}, and c_b; those that for plates that apply are P_x, P_{xc}, and P_{xc}/P_{xc}. See Footnote 14, page vii, for definitions.

Table 3 (Concluded)

Test No.	Standard Penetration Resistance C_s, kPa	Coil Penetration Resistance Force P_x, N	Average Penetration Resistance C_x or P_x (F/A_x), kPa	Penetration Resistance Ratio C_{xs} or P_{xs}	Penetration Velocity V_x cm/sec	Velocity Ratio $(V/l)_{xs}$	Apparent Coefficient of Viscosity Ratio C_{xs} or P_{xs} : $(V/l)_{xs}$
			1.04- by 1.04-cm, 1.08-cm²-Base-Area, Flat (1:1) Plate				
3C-1-12-4	420	3.4	510	1.244	111	25.3	0.045
33-1-12-5	701	737	988	1.403	303	71.5	0.013
60-1-12-6	305	321	493	1.353	1124	261	1.00523
10-1-12-7	305	394	243	1.496	1136	264	0.00549
			2.04- by 2.08-cm, 4.24-cm²-Base-Area, Flat (1:1) Plate				
39-1-13-2	157	314	122	0.777	0.02	1.05	0.740
40-1-13-3	178	95	175	0.982	111	12.4	0.077
69-1-13-4	162	135	227	1.475	117	117	0.012
			7.04- by 7.04-cm, 50.1-cm²-Base-Area, Flat (1:1) Plate				
33-1-14-2	117	767	138	0.841	0.4	0.039	1.34
40-1-14-3	172	116	169	1.14	150	9.05	0.1
15-1-14-4	192	114	9	1.420	105	0.42	0.012
			1.04- by 2.04-cm, 2.03-cm²-Base-Area, Flat (1:) Plate				
16-1-15-4	64	177	15	1.336	2.84	54	0.015
26-1-15-2	4	43	1057	1.215	116	3.4	0.0422
73-1-15-3	74	550	1111	1.491	334	173	0.0129
3-1-15-4	701	56	477	1.462	1604	349	0.00407
44-1-15-7	541	4	891	1.29	1.04	223	0.00247
			3.49- by 7.1-cm, 25.4-cm²-Base-Area, Flat (1:) Plate				
4-1-16-2	568	1371	431	1.045		0.977	1.070
35-1-16-4	4	14	391	1.247	111	1.47	0.0759
65-1-16-5	153	479	773	1.493	1107	170	0.0114
			4.30- by 10.72-cm, 551.1-cm²-Base-Area, Flat (1:) Plate				
56-1-17-2	20	347	4	1.47	4.4	0.534	0.047
57-1-17-4	5	7629	604	1.37	1.4	4.35	0.150
			4.47- by 5.04-cm, 6.45-cm²-Base-Area, Flat (1:) Plate				
21-1-1-4	47	34	424	1.44	4.5	2.65	0.045
31-1-1-3	4	34	7	1.20	4.4	1.45	0.14
31-1-1-4	45	443	449	1.21	165	1.43	0.028
40-1-1-5	4	4	730	1.34	5.7	7.4	0.17
9-1-1-4	4	4	45	1.41	22	4.1	0.4
44-1-1-7	445	4	433	1.37	17	4.4	0.0444
			1.04- by 1.04-cm, 1.04-cm²-Base-Area, Flat (1:) Plate				
4-1-4		4	424	1.42	174	1.47	7.
3-1-1-4	947	1.74	41	1.131	912	4.4	0.11
7-1-4-4	174	4	4	1.41	4	14	0.11
			4.04- by 4.04-cm, 24.4-cm²-Base-Area, Flat (1:) Plate				
4-1-4	47	44	4	1.243	4	4	1.45
4-1-4	47	4	4	1.14	4	4	0.1
4-1-4	4	14	4	1.45	4	4	0.177
			1.04- by 1.04-cm, 1.04-cm²-Base-Area, Flat (1:) Plate				
4-1-4		4	47	1.42	4.4	4	7.
4-1-4-3	47		47	1.44	4.4	4	4
4-1-4	4	4	44	1.44	4	4	7.4
4-1-4	4	4	47	1.404	4	4	0.4
4-1-4	4	4	4	1.211	144	4	0.47
4-1-4	4	4	4	1.47	44	44	1
			1.04- by 1.04-cm, 1.04-cm²-Base-Area, Flat (1:) Plate				
4-1-4	4	1.4	44	1.41	7.4	1.1	0.47
4-1-4	1.44		14	1.14	11	14.7	0.47
4-1-4	4			1.47	4	4	0.44
			1.04- by 1.04-cm, 1.04-cm²-Base-Area, Flat (1:) Plate				
4-1-4	4	47		1.4		4	1.44
4-1-4	44	41		44		4	4.1
4-1-4	44	1447				4	4.4

55

a. LENGTH TO WIDTH BASE RATIO, 1:1

$P_{XS} = 0.80(V/\ell)_{XS}^{0.100}$

b. 1:2

$P_{XS} = 0.80(V/\ell)_{XS}^{0.100}$

c. 1:4

$P_{XS} = 0.80(V/\ell)_{XS}^{0.100}$

d. 1:8

$P_{XS} = 0.80(V/\ell)_{XS}^{0.100}$

PENETRATION RESISTANCE RATIO P_{XS}

VELOCITY RATIO $(V/\ell)_{XS}$

LEGEND

BASE AREA,
SQ CM

o	1.61
△	3.23
□	6.45
o	12.9
◇	25.8
▽	58.1

NOTE. OPEN SYMBOLS DATA FROM SOIL
CARS OF AVERAGE C_S VALUES
210 AND 290 KPa

CLOSED SYMBOLS DATA FROM SOIL
CAR OF AVERAGE C_S VALUE 809 KPa

RELATION OF PLATE
PENETRATION RESISTANCE
RATIO TO VELOCITY RATIO
LOG PLOTS
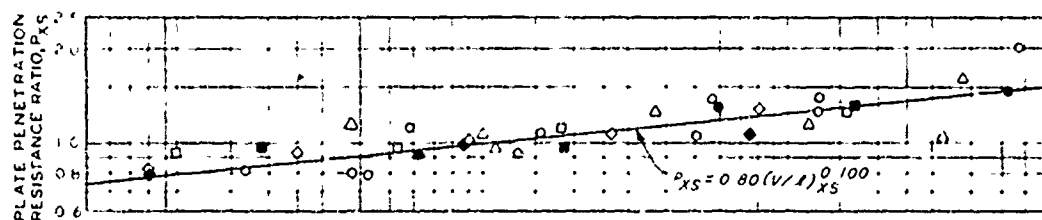95-PERCENT-SATURATED
FAT CLAY
FLAT RECTANGULAR PLATES

PLATE 1

INFLUENCE OF VISCOSITY
ON PENETRATION RESISTANCE
OF FAT CLAY TO
RECTANGULAR PLATES

LOG PLOT

95-PERCENT-
SATURATED FAT CLAY

LEGEND

O I I PLATES, ALL SIZES
△ I 2 PLATES, ALL SIZES
□ I 4 PLATES, ALL SIZES
◇ I 8 PLATES, ALL SIZES

NOTE OPEN SYMBOLS DATA FROM SOIL
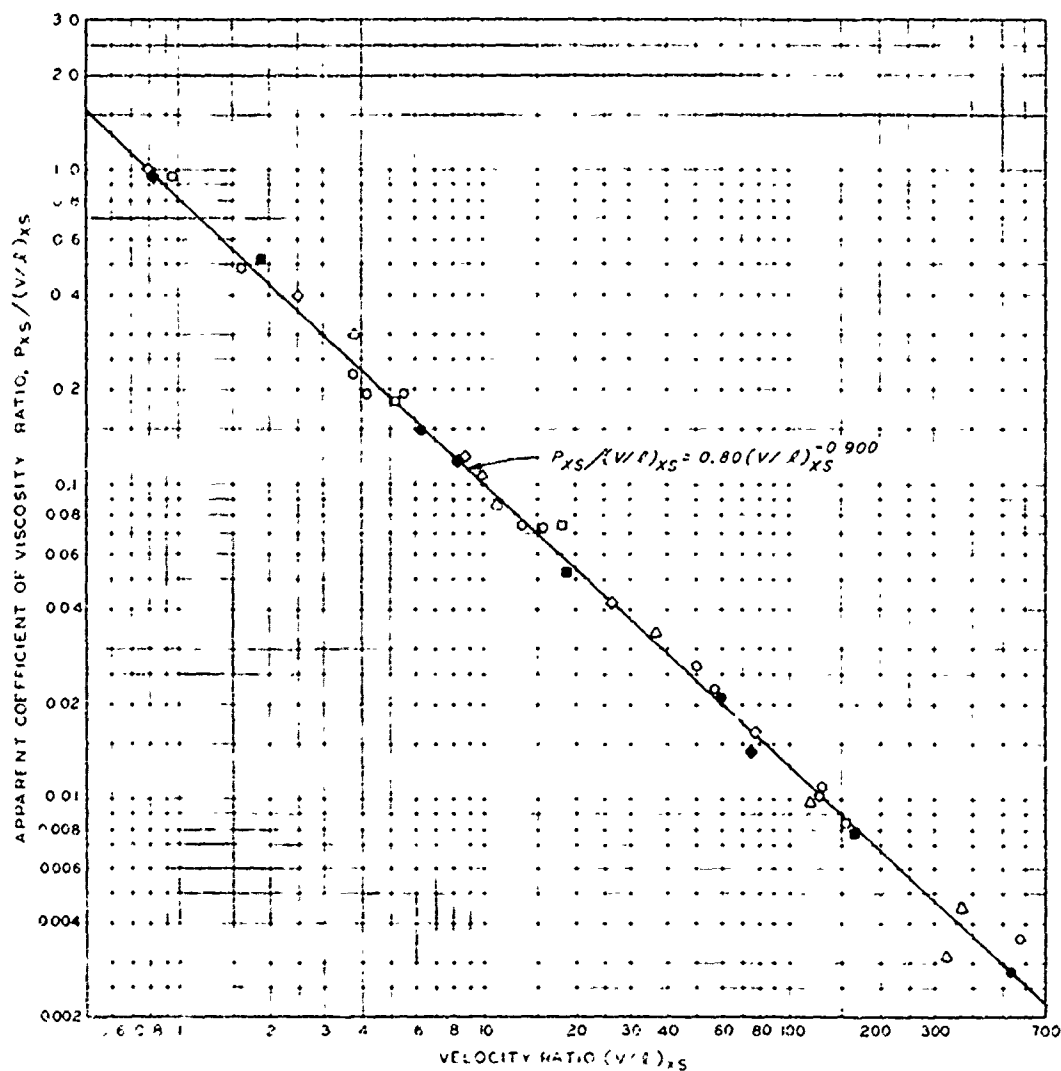CARS OF AVERAGE C_S VALUES
210 AND 290 KPa

CLOSED SYMBOLS DATA FROM SOIL
CAR OF AVERAGE C_S VALUE 809 KPa

$$P_{XS}/(V/\ell)_{XS} = 0.80(V/\ell)_{XS}^{-0.900}$$

PLATE 2   58

a.

Plate penetration resistance ratio, P_{XS}

$P_{XS} = 0.80(V/\ell)_{XS}^{0.100}$

b.

Apparent coefficient of viscosity ratio, $P_{XS}/(V/\ell)_{XS}$

$P_{XS}/(V/\ell)_{XS} = 0.80(V/\ell)_{XS}^{-0.900}$
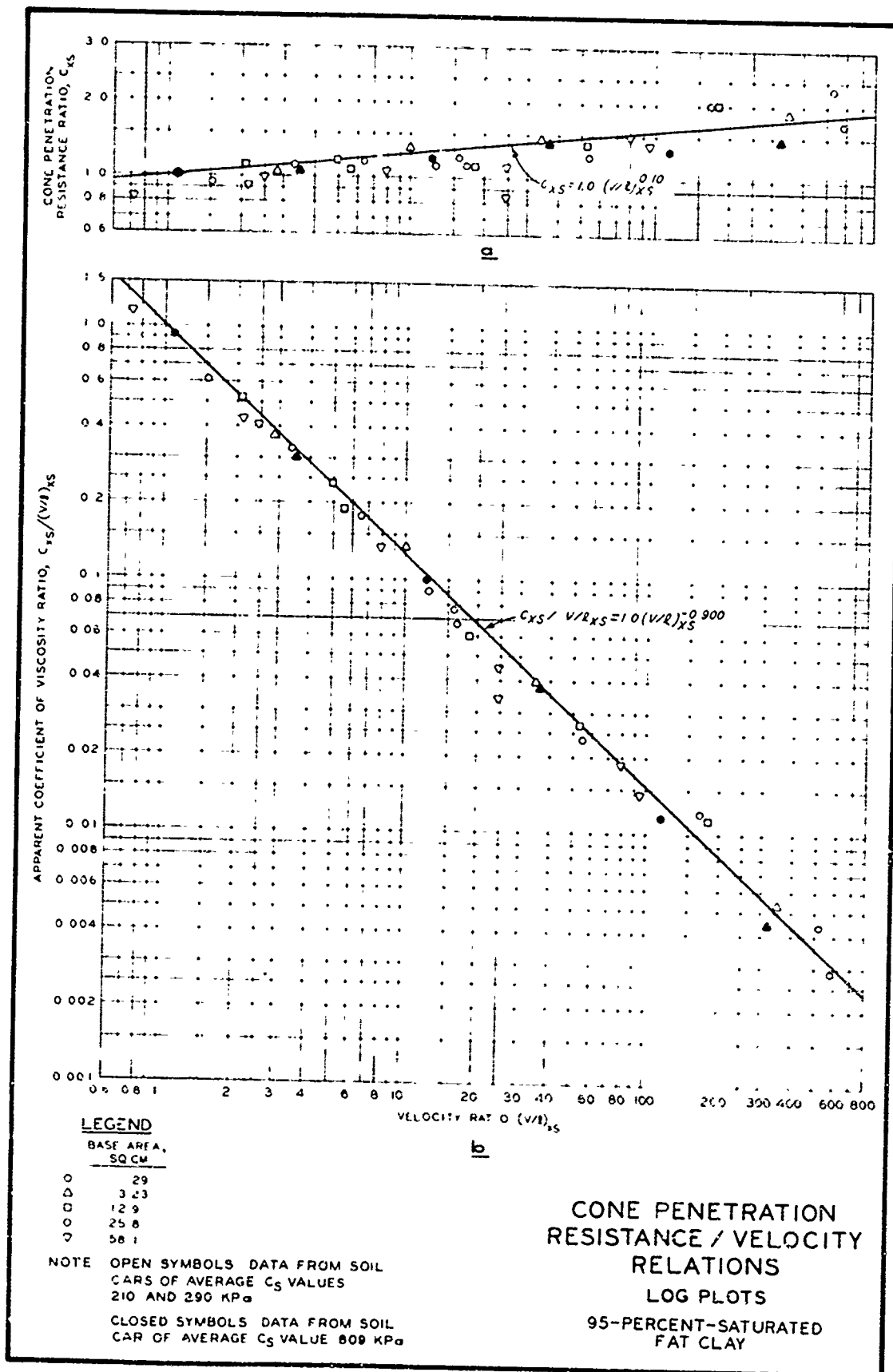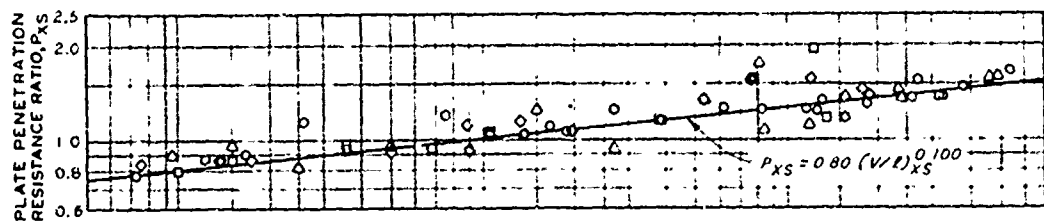
VELOCITY RATIO $(V/\ell)_{XS}$

LEGEND

BASE AREA,
SQ CM
1 29
3 23
12 9
25 8
54 1

NOTE   N SYMBOLS DATA FROM SOIL
CARS OF AVERAGE c_S VALUES
210 AND 290 KPa

CLOSED SYMBOLS DATA FROM SOIL
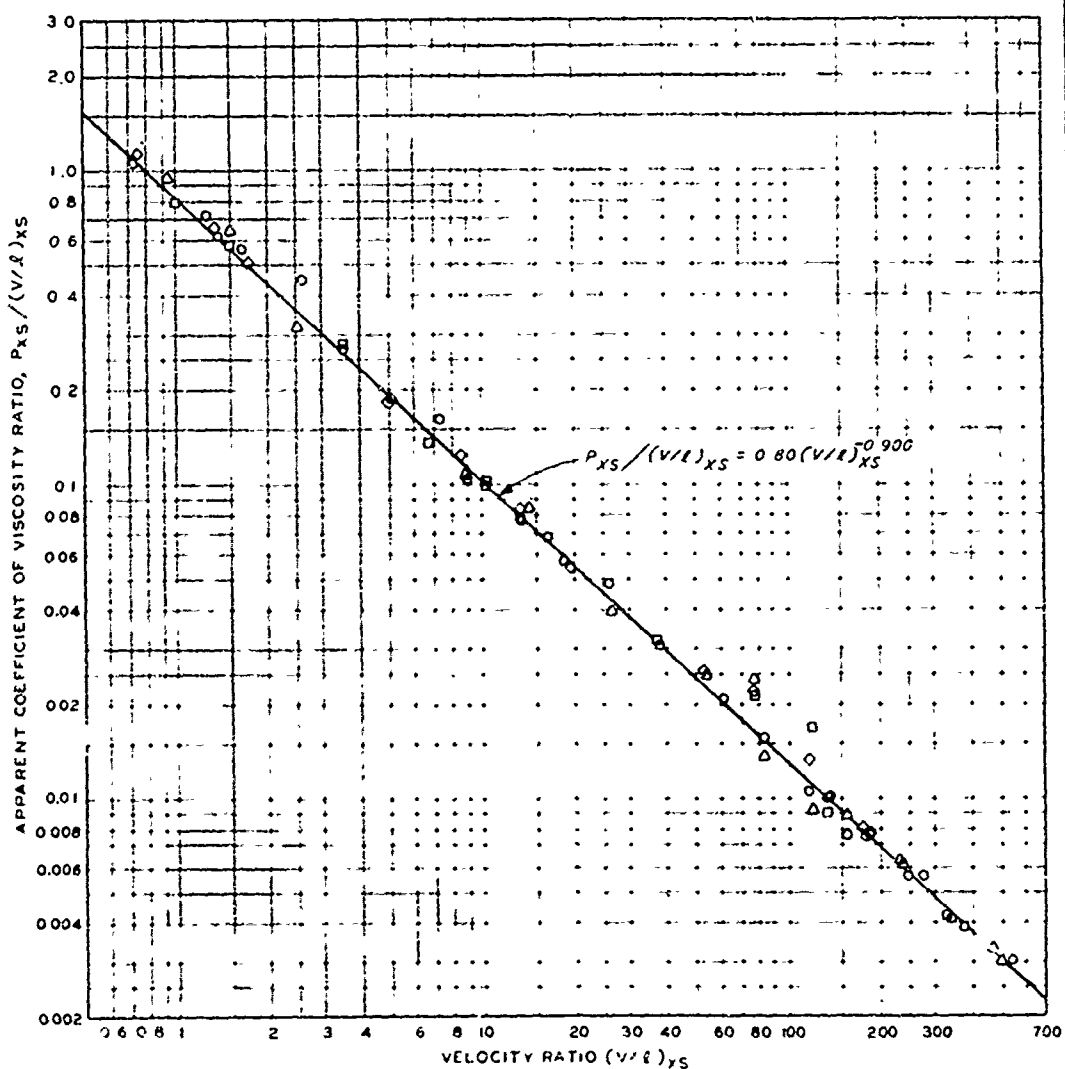CAR OF AVERAGE c_S VALUE 809 KPa

CIRCULAR PLATE
PENETRATION
RESISTANCE/VELOCITY
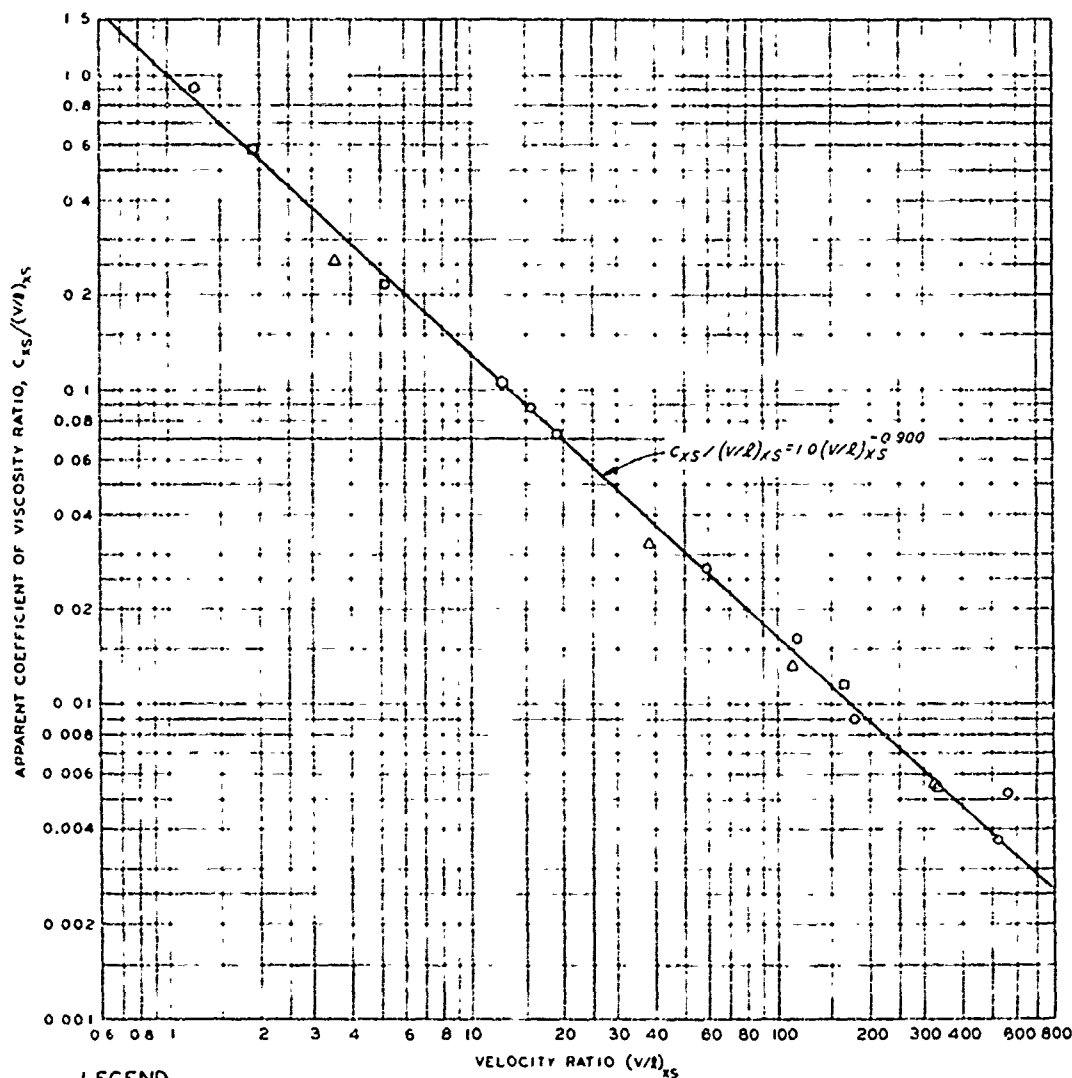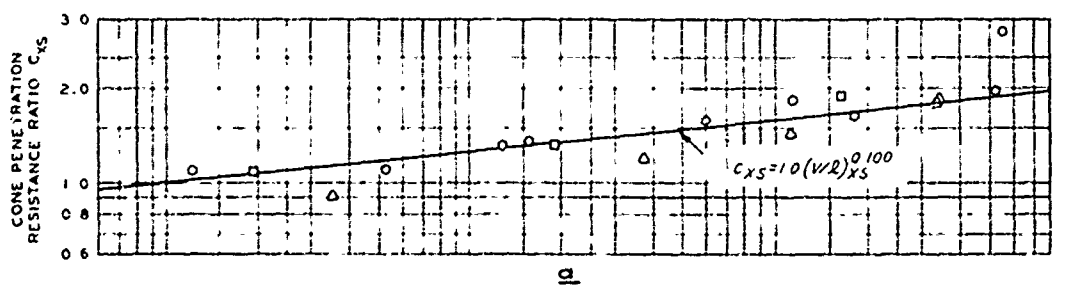RELATIONS

LOG PLOTS
95-PERCENT-SATURATED
FAT CLAY

CONE PENETRATION
RESISTANCE / VELOCITY
RELATIONS

LOG PLOTS

95-PERCENT-SATURATED
FAT CLAY

PLATE 4

60

a.

Plate penetration resistance ratio, P_{XS} (vertical axis, 0.6 to 2.5); Velocity ratio (horizontal).

$P_{XS} = 0.80 \, (v/\ell)_{XS}^{0.100}$

b.

Apparent coefficient of viscosity ratio, $P_{XS}/(v/\ell)_{XS}$

$P_{XS}/(v/\ell)_{XS} = 0.80 \, (v/\ell)_{XS}^{-0.900}$

VELOCITY RATIO $(v/\ell)_{XS}$

LEGEND

o	CIRCULAR PLATES, ALL SIZES
△	1:1 PLATES, ALL SIZES
⊐	1.2 PLATES, ALL SIZES
o	1.4 PLATES, ALL SIZES
◇	1.8 PLATES, ALL SIZES

PLATE PENETRATION
RESISTANCE/VELOCITY
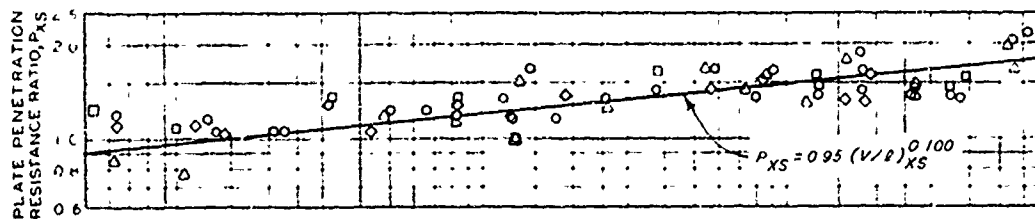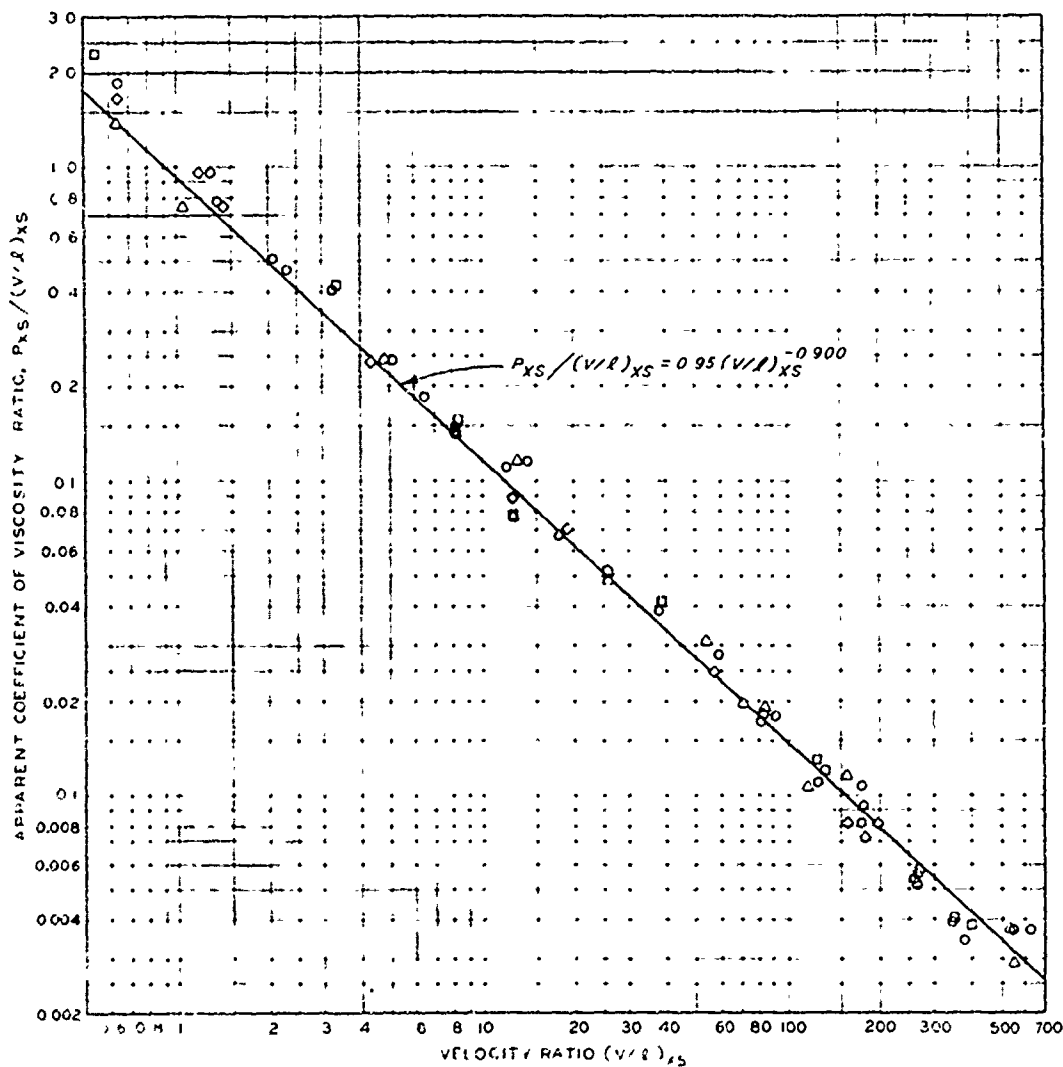RELATIONS

LOG PLOTS

90-PERCENT-SATURATED
LEAN CLAY

61

PLATE 5

CONE PENETRATION
RESISTANCE / VELOCITY
RELATIONS

LOG PLOTS

90-PERCENT-SATURATED
LEAN CLAY

PLATE 6

62

PLATE PENETRATION RESISTANCE / VELOCITY RELATIONS

LOG PLOTS

90-PERCENT-SATURATED SILT

PLATE 7

CONE PENETRATION
RESISTANCE / VELOCITY
RELATIONS
LOG PLOTS
90-PERCENT-SATURATED SILT

PLATE 8

64

APPARENT COEFFICIENT OF VISCOSITY RATIO, $c_{xs}/(v/\ell)_{xs}$

$$c_{xs}/(v/\ell)_{xs} = 10(v/\ell)_{xs}^{-0.900}$$

a. LOG PLOT

CONE PENETRATION RESISTANCE RATIO, c_{xs}

$$c_{xs} = 10(v/\ell)_{xs}^{0.100}$$

VELOCITY RATIO $(v/\ell)_{xs}$

b. ARITHMETIC PLOT

LEGEND

o FAT CLAY
Δ LEAN CLAY
□ SILT

CONE PENETRATION
RESISTANCE/ VELOCITY
RELATIONS

THREE 90-PERCENT-SATURATED,
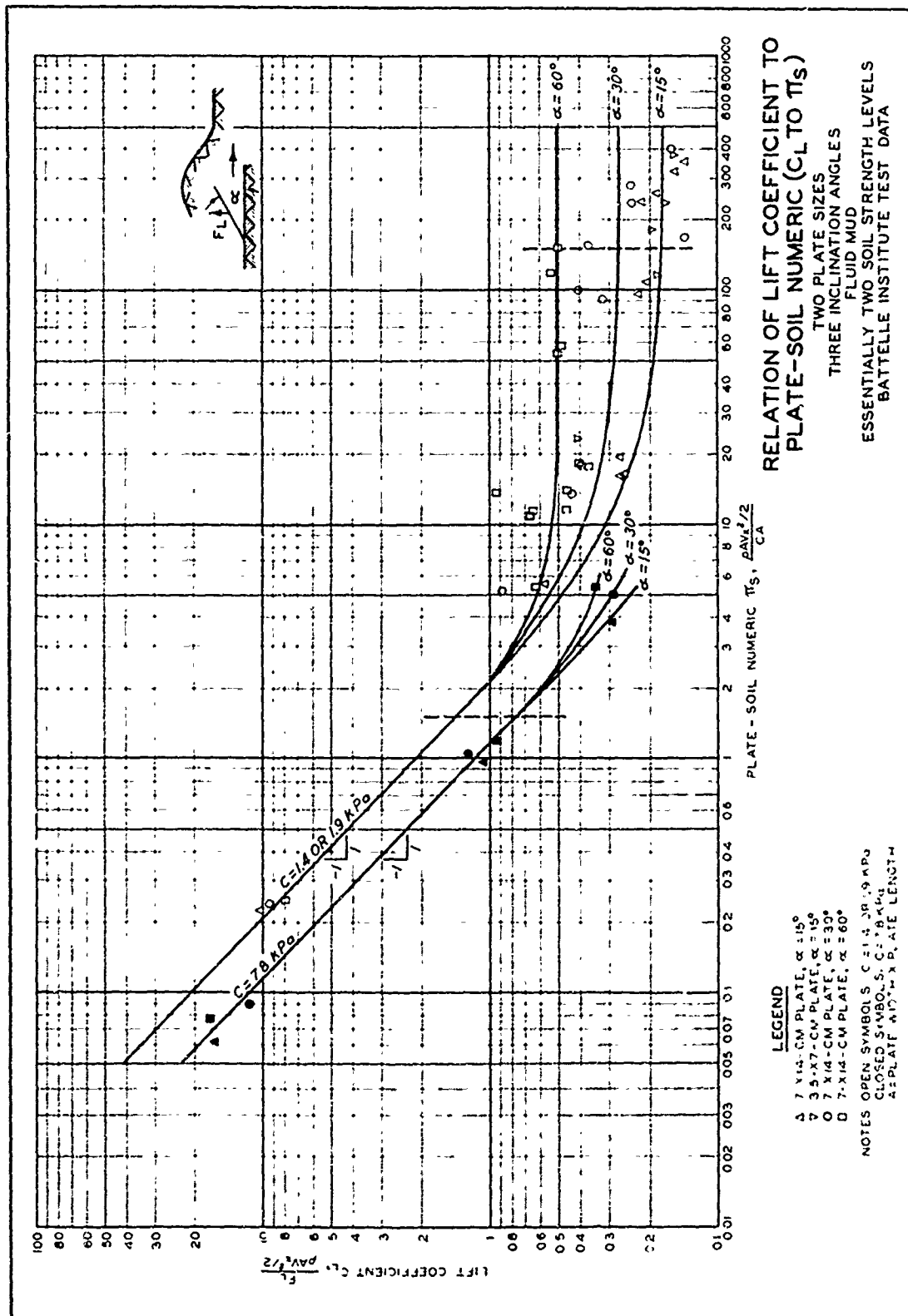FINE-GRAINED SOILS

0 323-SQ-CM-BASE-APEX CONE

RELATION OF LIFT COEFFICIENT TO
PLATE-SOIL NUMERIC (C_L TO π_S)
TWO PLATE SIZES
THREE INCLINATION ANGLES
FLUID MUD
ESSENTIALLY TWO SOIL STRENGTH LEVELS
BATTELLE INSTITUTE TEST DATA

PLATE 10

99

RELATION OF LIFT COEFFICIENT TO
PLATE-SOIL NUMERIC (C_L TO π_S)
TWO PLATE SIZES
(PROJECTED AREA USED IN INERTIAL FORCE TERM)
THREE INCLINATION ANGLES
FLUID MUD
ESSENTIALLY TWO SOIL STRENGTH LEVELS
BATTELLE INSTITUTE TEST DATA